THE
PHYSICAL REVIEW
A Journal of Experimental and Theoretical Physics Established by E. L. Nichols in 1893
VOL. 59, NO. 6 MARCH 15, 1941 SECOND SERIES

# The Continuous X-Rays Excited by the Beta-Particles of $_{15}P^{32}$

CHIEN-SHIUNG WU
*Radiation Laboratory, Department of Physics, University of California, Berkeley, California*
(Received January 24, 1941)

The internal and external x-rays (innere and äussere bremsstrahlung) excited by the beta-particles of $_{15}P^{32}$ were investigated by means of a Freon-filled ionization chamber connected to a sensitive d.c. amplifier. The intensity of the internal x-rays excited by the disintegration electrons when leaving the nucleus was found by the extrapolation method to be approximately equal to one-fourth of that of external x-rays excited by completely stopping the electrons in aluminum. From the experimental data the total energies of the two radiations were estimated. For internal x-rays this estimate leads to about 0.0020 $mc^2$ per disintegration electron, and for the external x-rays excited in aluminum to about 0.0082 $mc^2$. On the other hand, by making use of Lyman's magnetic beta-spectrum of $_{15}P^{32}$ the energy of internal x-rays calculated from the theory of Knipp and Uhlenbeck was 0.0020 $mc^2$ per disintegration electron and the energy of the external x-rays expected from the theory of Bethe and Heitler was 0.0089 $mc^2$. Therefore the experimental results are in good accord with the theoretical predictions. The relation between the intensity of the external x-rays excited by completely stopping electrons in Pb, W, Sn, Ag, Mo, Cu, Fe, Al, C and Be and the atomic number was investigated. It was found to be in fairly good agreement with the theoretical curve derived according to Bloch's formula for energy loss of electrons by inelastic collisions (F. Bloch, Ann. d. Physik **16**, 285 (1933); Zeits. f. Physik **81**, 363 (1933)) and the theory of Bethe and Heitler, namely that the intensity is proportional to the square of the atomic number. From the shape of the absorption curves of the total x-rays it will be seen that the spectral distribution of the external x-rays is independent of $Z$ (atomic number) and is also approximately the same as that of the internal x-rays.

## I. INTRODUCTION

THE disintegration of most beta-radioactive substances is accompanied by the emission of gamma-rays. The gamma-rays are highly monochromatic and may produce a secondary beta-ray emission due to a photoelectric effect of the gamma-quantum on an electron of the disintegrating atom itself. However, there are certain beta-emitting nuclei which not only give a normal continuous electron spectrum, but also emit no monochromatic gamma-rays. Nevertheless there are always fairly weak inhomogeneous gamma-rays accompanying this kind of disintegration. This was first observed by Aston[1] in his measurements on RaE and since then it has been repeatedly investigated in different laboratories.[2] The most probable interpretation of this inhomogeneous low intensity gamma-radiation is the one in which the radiation is considered as secondary in origin, emitted by the changing dipole moment of the atom when the electronic charge is suddenly shifted from the nucleus to a region outside, by the emission of a beta-particle. The whole theory of this process, known as

[1] G. H. Aston, Proc. Camb. Phil. Soc. **23**, 935 (1927).

[2] S. Bramson, J. de phys. et rad. **66**, 721 (1930); E. Stahel and D. J. Conmore, Physica **2**, 707 (1935); G. J. Sizoo and D. J. Conmore, Physica **3**, 921 (1936); E. McMillan, Phys. Rev. **47**, 801 (1935); G. V. Droste, Zeits. f. Physik **100**, 529 (1936); G. J. Sizoo, C. Eickman and P. Green, Physica **6**, 1057 (1939); E. Stahel and J. Guillessen, J. de phys. et rad. **1**, 12 (1940).

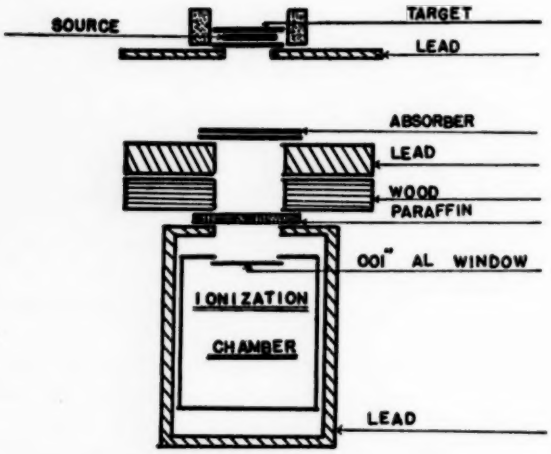


FIG. 1. Experimental arrangement.

internal x-rays (*innere* bremsstrahlung) has been worked out recently by Knipp and Uhlenbeck.[3]

On the other hand, when an electron passes through the electrostatic field of a nucleus, it is generally deflected. Since this deflection always produces a certain acceleration, the electron, according to the classical theory, must emit radiation. In the quantum theory, there will be a certain probability that a light quantum $K$ is emitted, the electron making a transition to another state. This is usually called the external x-rays (*äussere* bremsstrahlung) to contrast with the internal x-rays (*innere* bremsstrahlung) and its rate of production has been calculated by Bethe and Heitler.[4]

The radiation loss becomes an appreciable amount at energies of several million volts. The availability of strong sources of artificial radioactive substances in this laboratory has made it possible to test their prediction. $_{15}P^{32}$ has been chosen for this purpose because it emits beta-particles with a maximum energy of 1.7 Mev and no gamma-rays. Its slow decay, of half-life 14.30 days, makes it particularly suited for this investigation. Moreover, the theoretical calculation by Knipp and Uhlenbeck is based on the assumption that the influence of the nuclear charge on the electron emitted can be neglected. $_{15}P^{32}$ has a rather small nuclear charge ($Z=15$); therefore it has another advantage so far as this requirement is concerned.

[3] J. K. Knipp and G. E. Uhlenbeck, Physica **3**, 425 (1936).

[4] H. Bethe and W. Heitler, Proc. Roy. Soc. **146**, 83 (1934).

The purpose of this investigation is to attempt to arrive at some conclusions as to whether this inhomogeneous gamma-radiation of low intensity from $_{15}P^{32}$ is entirely due to the secondary effect, namely, the radiation loss of the fast electrons coming out of the nuclei, or only partly due to it, the rest originating directly in the nucleus. It is also an intention of this work to make a comparison of the quantum yield between experimental results and theoretical predictions.

## II. Experimental Procedure

The radioactive $_{15}P^{32}$ (of an order of 5 millicuries) was activated by bombarding phosphorus with deuterons on an inner target[5] in the Berkeley cyclotron. Since phosophorus prepared in this way always contains some impurities, especially Mn, Fe and Co, in order to make sure that the gamma-rays from these impurities are no longer present, a very extensive chemical purification by repeated precipitations in alkaline and acid solutions was first carried out. The phosphate solution was warmed in a water bath and the sulfate molybdate reagent then added and shaken. The solution was allowed to stand not less than several hours. Then the precipitate was filtered on a calcium filter and carefully washed with 2 percent ammonium nitrate. After having been thoroughly washed, the precipitate was again dissolved by pouring ammonium hydroxide through the filter, and acidified with nitric acid. Since the phospho-molybdate precipitation is effective in recovering the phosphorus free of contaminants, the process was repeated several times. Finally, the phosphorus was precipitated down as magnesium ammonium phosphate by adding magnesia mixture to the ammonia solution. The magnesium ammonium phosphate thus obtained was again converted into magnesium pyrophosphate which was then evenly spread on extremely thin Cellophane (1.5 mg/cm$^2$) and framed in a light cardboard ring in order to avoid as much as possible any external x-rays excited from the mounting.

The measurements were carried out by an ionization chamber which was made of steel, lined on the inside with cardboard, and the inner

[5] R. R. Wilson and W. D. Kamen, Phys. Rev. **54**, 1031 (1938).

cylinder was a fine steel cage of 10-cm diameter and height. It was filled with Freon ($CCl_2F_2$), slightly above atmospheric pressure. The window was aluminum of 7 mg/cm² thickness. The ionization chamber was completely shielded with 3 cm of lead and connected to a sensitive d.c. amplifier of the type modified by DuBridge.[6]

## III. Measurements

### (a) The absorption of the beta-rays in aluminum

An absorption curve of the beta-rays from $_{15}P^{32}$ in aluminum has been carefully measured. The experimental arrangement is shown in a schematic diagram (Fig. 1). No paraffin is in front of the window for measuring the absorption of the beta-rays. The grid current in the circuit was always balanced by adjusting the background current which was in turn adjusted by varying the distance of a weak radium source from the ionization chamber. A glance at the absorption curve (Fig. 2) reveals that after the electrons have been completely absorbed, a feeble yet penetrating radiation still remains. Its intensity amounts to only one four-thousandth of that of electrons. The part of the absorption curve beyond a thickness of an absorber of 500 mg/cm² appears to follow an exponential law. This straight part may be extended to intersect the line representing gamma-ray intensity in order to give an end point, which reads 780 mg/cm². According to the empirical formula of Feather[7] this value corresponds to energy of 1.72 Mev, which is in good accord with Lyman's[8] accurate result (1.69 Mev) determined by the magnetic spectrograph method.

### (b) The absorption of x-rays excited in different materials by beta-particles from $_{15}P^{32}$

The experimental arrangement is the same as in Fig. 1. The electron source which consists of an extremely thin layer of $_{15}P^{32}$ was placed between two pieces of metal which served as targets. Then a wall of paraffin, having a thickness of 1.5 cm, was used to encircle the source in order to make sure no beta-particle could come out. The thickness of the metal under investigation was so chosen that it was just enough to stop all the electrons. The geometrical condition was excellent. The ionization chamber and source were 12 cm apart, and the absorbers were always situated midway between them. However, in order to assure the reliability of the coefficient of absorption calculated under these conditions, auxiliary experiments were also performed. One was to check the absorption coefficient of annihilated gamma-radiation from $Cu^{61}$ under exactly the same conditions. In this case it gave a value of $\mu_{Pb}=1.73$ cm$^{-1}$, which was in good agreement with the value $\mu_{Pb}=1.73$ cm$^{-1}$ stated in Gentner's[9] paper. The second method was to increase the distance between the source and chamber to 18 cm. If any radiation scattered from the absorbers had gotten into the chamber, then by altering the geometrical condition, it would have shown a noticeable difference in these two absorption curves (Fig. 3). In fact, no appreciable difference was detected.

From the parallel parts of these absorption curves (Fig. 4) it may be concluded that the

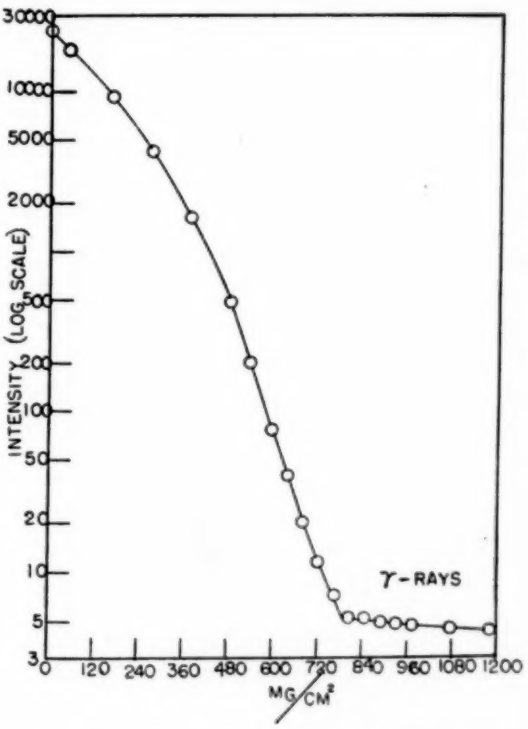


FIG. 2. Absorption in aluminum of the beta-particles from $_{15}P^{32}$.

[6] L. A. DuBridge and H. Brown, Rev. Sci. Inst. **4**, 532 (1933).
[7] N. Feather, Proc. Camb. Phil. Soc. **34**, 599 (1938).
[8] E. M. Lyman, Phys. Rev. **51**, 1 (1937).
[9] W. Gentner, Phys. Rev. **51**, 1 (1937).

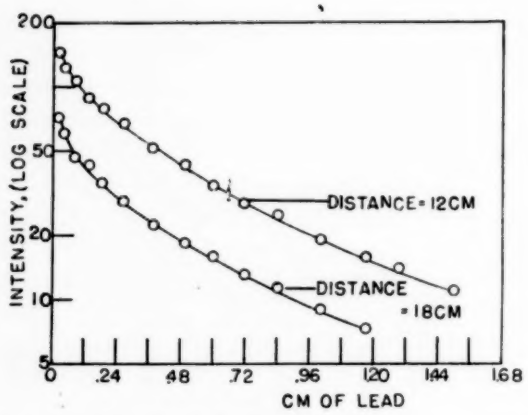


FIG. 3. Absorption in lead of the internal x-rays of $_{15}P^{32}$ plus the external x-rays excited in lead by beta-particles from $_{15}P^{32}$ under two different geometrical conditions.

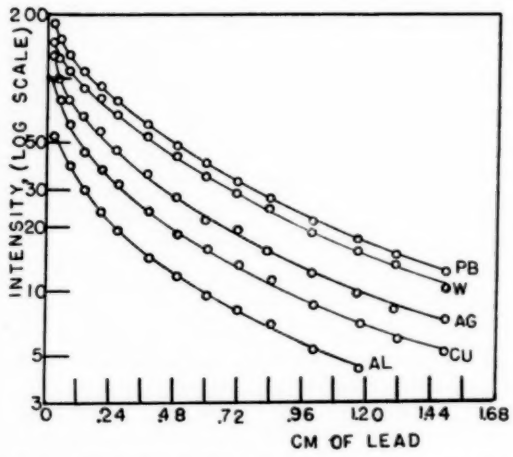


FIG. 4. Absorption in lead of the internal x-rays of $_{15}P^{32}$ plus the external x-rays excited in different metals by beta-particles from $_{15}P^{32}$.

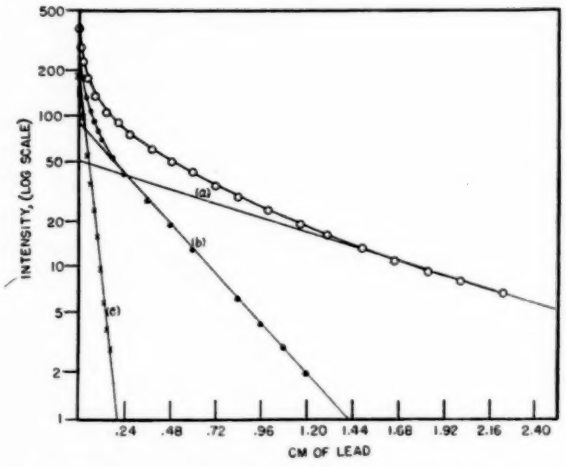


FIG. 5. Analyzed absorption curve in lead of the internal x-rays plus the external x-rays excited in aluminum. The mass absorption coefficient for curve (*a*) is 0.0952, for curve (*b*) is 0.278, for curve (*c*) is 2.30.

energy distribution of the harder part of the x-rays excited in different metals by fast electrons are more or less the same. The irregularities shown at the beginning of each curve seem to be justified by interpreting them as due to the unequal self-absorption in different targets.

Although the absorption curve of the x-rays shows definitely that the distribution of energy is continuous, if one takes any one of them, for instance, the absorption curve of x-rays excited in Al (900 mg/cm²), (Fig. 5) and proceeds by the ordinary method of analyzing an absorption curve, it can be shown that the curve is quite well represented by a resultant of three exponential curves *a*, *b*, *c* (Fig. 5) which have mass absorption coefficients, 0.0952, 0.278, and 2.30, respectively. In other words, the corresponding energies of these effective components are roughly 880, 370, and 160 kev. The apparent ratio of intensity among them is approximately 1 : 1.76 : 3.6. It is important to emphasize that the method of analyzing the absorption curve into three components is only a means by which the average energy per quantum may be estimated. Certainly it does not imply that there are only three components of x-rays existing. From these data, the average energy per quantum calculated is around 330 kev, but it must be borne in mind that this is only true when the sensitivity of the chamber responding to gamma-rays of different energies is the same. Otherwise the ratio must be subjected to correction. Unfortunately neither ionization chamber nor counter can ever fulfill this requirement; and, up to date, there is little known about the correlation between them.

### (c) The relation between the intensity of x-rays excited and the atomic number

According to the theoretical calculation by Bethe and Heitler, the intensity of x-rays excited by the beta-particles is proportional to the square of the atomic number $Z$. However, the number of nuclei encountered by an electron in passing through a metal before it is completely stopped is roughly inversely proportional to the atomic number of the stopping material. (For details

see IV (b), theoretical calculation for external x-rays.) Therefore, the intensity of x-rays excited by completely stopping electrons in a metal would be expected to be approximately proportional to the atomic number. Owing to the unequal self-absorption in the target, as shown in the absorption curves, it was necessary to put a certain thickness of lead in front of the chamber to minimize this effect. A piece of lead of 8000 mg/cm² thickness was used. It gave a curve slightly convex towards the abscissa axis (curve C, Fig. 6). If the curve is extended to intersect the ordinate axis, then the intercept will give the value of the intensity of internal x-rays. However, it is difficult to get very strong artificial radioactivity in a mono-atomic layer of small area. So long as the sample has a finite thickness, obviously the intercept will not give the true value of the intensity of internal x-rays, but rather the sum of the internal x-rays and the external x-rays excited in the sample itself. Nevertheless, there are still ways to correct this small amount of external x-rays excited in the sample itself. The method employed here is based on the experimental fact that the external x-rays excited from thin foils is approximately proportional to its mass per square centimeter. In other words, the ascending curve of the intensity of the external x-rays plotted against the mass per square centimeter is a fairly straight line near the origin.

Therefore inactive phosphate was prepared and was carefully made into two thin pieces, each of which had a thickness of 20 mg/cm², exactly equal to half of that of the active sample. The pieces were then placed adjacent to each side of the sample to double its thickness. Another series of measurements of the intensity against the atomic number of the stopping material was made. The results are shown in curve D. The intensity of the x-rays excited in aluminum was not appreciably altered by increasing the thickness of the sample. This may be explained by the fact that the atomic number of aluminum is approximately equal to the equivalent atomic number of the sample.* But those excited from the materials whose atomic numbers are either greater or smaller than that of aluminum were decreased or increased, respectively, as the thickness of the sample was doubled. The difference between the two readings which were taken before and after increasing the thickness of the sample gives the difference of the intensity between that excited in the metal and that in the sample. If the differences thus obtained are added to the corresponding points for those elements having an atomic number larger than that of aluminum and subtracted from its corresponding point for those elements lying below aluminum in the periodic table, then those points will represent the true values of the intensity of the total x-rays excited in different metals by the electrons from a mono-atomic layer. The curve passing through these points is shown in Fig. 6 as curve A, which shows that the internal x-rays have a value only one-fourth that of the external x-rays excited in aluminum.

One would naturally wonder why such an indirect estimation of internal x-rays has been used instead of using a direct and straightforward measurement by bending all the electrons away

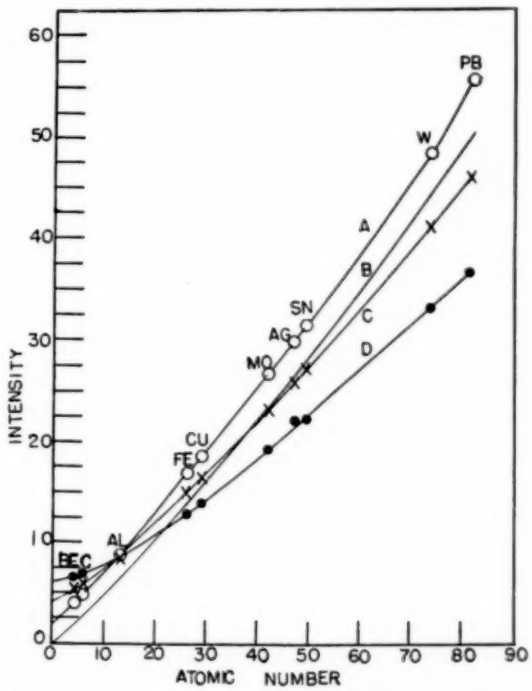


FIG. 6. The intensity of x-rays excited in different metals plotted against the atomic number. Curve A—Extrapolated curve for an infinitely thin sample; B—theoretically calculated curve; C—actually measured curve for a sample of a thickness of 40 mg/cm²; D—actually measured curve for a sample of a thickness of 80 mg/cm².

* The equivalent atomic number of the sample $Mg_2P_2O_7$ is 10.8.

in a strong magnetic field. The reason for doing this is that there are always unavoidable amounts of external x-rays excited on the pole faces and walls, part of which will be scattered into the chamber and therefore increase the uncertainty of the value of the internal x-rays. The direct method can perhaps be well carried out in case a very strong source is available, so that the conditions of proper collimating and shielding can be fulfilled.

**(d) The ratio between the number of electrons and x-rays excited**

In order to be able to compare the experimental results with the theoretical calculations, the ratio between the number of electrons and the x-ray quantum excited must be known. This was roughly estimated by measuring the ionization ratio between the electrons and x-rays excited in aluminum in the ionization chamber, and gave a value of 4050. For comparison, the ionization ratio between the positrons and the annihilation radiation of $Cu^{61}$ was determined under exactly the same condition and the value 45 was found. Since there are two annihilation gamma-rays per positron which enter the chamber, the ratio between one electron and one gamma-quantum will be approximately 90. Since the beta-rays from $_{15}P^{32}$ are slightly more penetrating than those from $Cu^{61}$, it seems advisable to apply a correction factor of about 50/68 [10] to the efficiency obtained from $Cu^{61}$. Therefore the ratio is 66. The correction for gamma-rays of different energies is rather difficult to estimate because it involves the wall effect which complicates the matter. If it is assumed that the ionization produced by x-rays is comparable to that by annihilation radiation, the number of x-ray quanta produced per electron is $66/4050=0.016$. This value times the average energy per quantum gives the average energy radiated in aluminum and source $0.016 \times 330 = 5.28$ kev per electron. Since the intensity of the internal x-ray is only one-fourth of that excited in aluminum, the average energy of internal x-rays excited per electron is $1.05/510 = 0.0020\, mc^2$. The external x-ray excited in aluminum is about $0.0082\, mc^2$.

[10] W. Wilson, Proc. Roy. Soc. **A85**, 240 (1911).

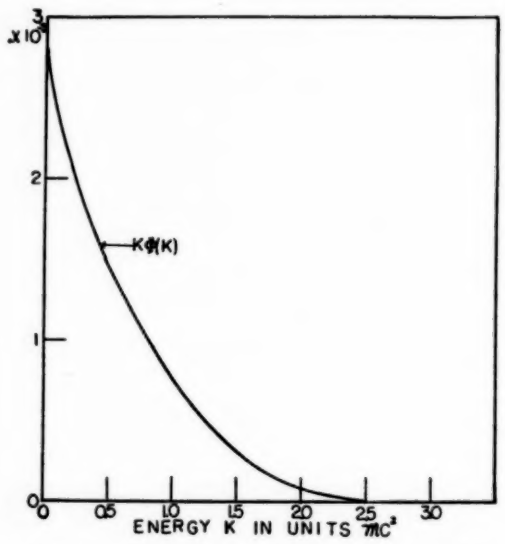


FIG. 7. $k\Phi(k)$ of the internal x-rays of $_{15}P^{32}$ as a function of the energy.

## IV. THEORETICAL CALCULATIONS

**(a) Internal x-rays (*innere* bremsstrahlung)**

According to Knipp and Uhlenbeck's theory of internal x-rays the probability that an electron, created with energy $W_e$ radiates a light quantum of energy $k$, is represented by

$$\phi=\frac{\alpha p}{\pi p_e k}\left[\frac{W_e^2+W^2}{W_e p}\log(W+p)-2\right] \qquad (1)$$

where $W$ is the energy of the electron after having given to the radiation field a quantum of energy $k$ or $W_e=W+k$. $P_e$ and $p$ are the momentum of the electron before and after the radiation occurred.

From Eq. (1) the distribution in energy of the x-ray radiation for a given initial electron energy can be plotted. The entire radiation spectrum $\Phi(k)$ for the whole distribution of electrons from $_{15}P^{32}$ can be obtained by multiplying the radiation probability $\phi$ for an electron of energy $W_e$ by $P(W_e)dW$, the probability of the emission of an electron with that initial energy $W_e$, and integrating over all values of $W_e$ from zero to the end point of the electron spectrum. The function $P(W_e)$ can be directly derived from Lyman's data on the momentum distribution of the electrons from $_{15}P^{32}$. For the present purpose the total x-ray intensity, $k\Phi(k)$, has been plotted in this way. It is shown in Fig. 7. The area under

the curve gives the energy of internal x-rays per electron as approximately $0.0020\ mc^2$.

The internal x-ray calculation used here involves two approximations. The first, neglect of the effect of the nuclear charge on the motion of the emitted electron, is justified in this case, where the parameter $Z\alpha$ is only $\sim 0.1$. The second is the assumption that the x-radiation and the electron emission are independent processes, justifying the calculation of the total x-radiation by the use of the observed electron spectrum. This assumption implies that the coupling between the heavy and light particles involved in beta-decay does not depend on the electron momentum.[11] Since the long lifetime of $_{15}P^{32}$ is interpreted as meaning that the transition involved is a "forbidden" one, involving the carrying away of one or more units of angular momentum by the emitted electron, the coupling here would be expected to be at least proportional to the electron wave-length. The close agreement with the simple theory is therefore rather unexpected, and may indicate that the coupling is not strongly dependent on electron wave-length, or merely that the integrated quantities measured are insensitive to changes in the spectrum of the radiation.

**(b) External x-rays (*äussere* bremsstrahlung)**

According to Bethe and Heitler's theory of external x-rays, the average energy lost in one collision may be obtained by integrating the intensity $k\phi_k$ over all frequencies from 0 to $W_e-\mu$ where $W_e$ is the energy of the electron and $\mu$ is equal to $mc^2$, the rest energy of the electron. Therefore this is

$$\int_0^1 k\phi_k d\left(\frac{k}{W_e-\mu}\right), \tag{2}$$

where $k$ is the energy of the quantum emitted, $\phi_k$ is the cross section for the emission of a quantum $k$.

$\phi_k$ is a rather complicated function of $k$; however, from the intensity distribution curve of the bremsstrahlung shown in Fig. 14 [12] (*The Quantum Theory of Radiation* by Heitler), one can see that for electrons of small energy, the distribution curve, except for the very soft radiation, can be roughly represented by a straight line. In this case, the average energy of the electrons coming from $_{15}P^{32}$ is around 680 kev. Therefore the function $\phi_k$ can be written as

$$k\phi_k \leqq 12\bar{\phi}W_e\left(1-\frac{k}{W_e-\mu}\right). \tag{3}$$

Substituting into Eq. (2)

$$\int_0^1 k\phi_k d\frac{k}{(W_e-\mu)} \leqq \frac{12\bar{\phi}W_e}{W_e-\mu}\int_0^{W_e-\mu}\frac{W_e-\mu-k}{W_e-\mu}dk \leqq 6\bar{\phi}W_e. \tag{4}$$

The average energy lost in the whole range can be obtained by integrating the value obtained in (4) over all collisions in the passage.

$$W_{\text{rad}} = 6N\bar{\phi}\int_0^{R_{max}} W_e dx. \tag{5}$$

But the radiation energy loss of an electron of 1 Mev in passing through a metal is small in comparison with the ionization energy loss, and therefore one can write

$$dx = \frac{dE}{(dE/dx)_{\text{ioniz}}}.$$

Assuming that the range-energy curve is nearly linear in this region, an average stopping power for an electron energy about one Mev is used.

Applying Eq. (5) on page 219 of reference 15 for $(dE/dx)_{\text{ioniz}}$ it gives

$$dx = \frac{dE}{13.2NZ\phi_0\mu(1+0.35\log_{10}(82/Z))} \tag{6}$$

for any atomic number $Z$.

Substituting (6) and (5) one gets

$$\begin{aligned} W_{\text{rad}} &= 6N\frac{r_0^2Z^2}{137}\frac{3}{8\pi r_0^2}\times\frac{1}{13.2NZ\phi_0\mu(1+0.35\log_{10}(82/Z))}\int_\mu^W W_e dW_e \\ &= 0.19\times10^{-4}\frac{Z}{\mu(1+0.35\log(82/Z))}(W^2-\mu^2) = \frac{Z\times0.19\times10^{-4}}{\mu(1+0.35\log(82/Z))}(pc)^2. \end{aligned} \tag{7}$$

[11] P. Morrison and L. I. Schiff, Phys. Rev. **58**, 24 (1940).
[12] W. Heitler, *Quantum Theory of Radiation* (Oxford University Press, 1936).

For aluminum, $Z=13$:

$$W_{\text{rad}}=\frac{Z\times 0.148\times 10^{-4}}{\mu}(pc)^2.$$

The average value of $(pc)^2$ for the entire electron spectrum of $_{15}P^{32}$ is evaluated from Lyman's result. It is equal to $4.63\mu^2$.

Therefore the average energy loss in aluminum is:

$$W_{\text{rad}}(\text{Average})=13\times 0.148\times 10^{-4}\times 4.63\mu$$
$$=0.0089mc^2.$$

Moreover, Eq. (7) derived above also gives the variation of the intensity of the external x-rays excited in different metals with the atomic number. Since the equation contains the atomic number not only in its numerator, but also involves the logarithm of the atomic number in its denominator, the intensity is expected to increase slightly more rapidly as the atomic number increases. The curve representing this theoretical relation between the intensity and the atomic number is shown in Fig. 6, curve B.

## Discussion

Although owing to the well-known difficulties encountered in the investigation of continuous energy spectra the results thereof always involve some uncertainties, quite a few satisfactory conclusions can be drawn from this information. The most interesting one is the intensity ratio between internal x-rays and external x-rays excited in different metals. According to the recent work of Sizoo and his collaborators,[13] the yield of internal x-rays is several times larger than expected from theoretical calculations. In the meantime they concluded that the yield of external x-rays excited by electrons in transversing metals is a few times smaller than predicted. The large discrepancies between their experimental results and theoretical calculation may be explained by the fact that part of the external x-rays excited on the pole faces and walls has gotten into the counter. Therefore the value of internal x-rays seems much too high.

A quantitative comparison between experimental and theoretical values is rather ambiguous because of the difficulties mentioned above. Nevertheless the energy distributions of these two radiations are analogous, so that the intensity ratio between them will not be influenced by the uncertainties introduced in assuming equal sensitivity of the chamber. In order to avoid complicating the experiment by the scattering from the pole faces of the magnet, an indirect method was used as stated above. This method gave a ratio of one to four between internal x-rays and external x-rays excited in aluminum, which is in excellent accord with the theoretical predictions.

When Bethe and Heitler worked out the theory of external x-rays in 1934, they had hoped that some day a strong artificial beta-emission radioactive substance which emits no gamma-rays might be available in order to test the theory. In the light of this investigation we may conclude that, first, the energy distribution of external x-rays excited is independent of the nature of the target used, but the intensity of the x-rays does vary with the atomic number of the target. It is proportional to the square of the atomic number. We may also say that the average quantum yield in this process is also of the predicted order of magnitude.

It is a great pleasure for the author to express her gratitude to Professor E. O. Lawrence for his suggestion of investigating this problem and his valuable guidance throughout the course of the work. She also wishes to acknowledge her special indebtedness to Professor E. McMillan for his encouragement and criticism which have made this investigation possible, and to Dr. M. Kamen for his help in preparing the strong samples.

[13] G. J. Sizoo, C. Eijkman and P. Green, Physica **6**, 1057 (1939).

# Interaction Experiments with Resonance Neutrons*

HENRY B. HANSTEIN**
*Columbia University, New York, New York*
(Received January 18, 1941)

A slow neutron collimator of good geometrical proportions with multiple shielding has been constructed especially for use with the cyclotron, and transmission measurements of high precision have been made with neutrons in well-defined regions of the energy spectrum. With the resonance filter method for defining the energy of the neutron beam, cross sections of selected elements were determined for the resonance neutrons of indium (~0.9 ev energy) and iodine (25–100 ev energy) as well as the cadmium absorption group (thermal energy). Measurements were made by following the induced resonance activities of very thin detectors with an ionization chamber—electrometer system. The experimental work consisted of (1) cross section measurements of selected elements for indium resonance neutrons; (2) investigation of interference effects; (3) measurement of the neutron-proton and neutron-deuteron interactions for indium resonance neutrons and comparison measurements with thermal neutrons; (4) measurement of the neutron-proton interaction for iodine resonance neutrons. The neutron-proton cross section was investigated in some detail to establish definitely the free neutron-proton interaction. The effects of molecular binding should be practically negligible at about 1-ev energy and this is indicated by the fact that the same value of the neutron-proton interaction was obtained for the indium and iodine resonance neutrons; *viz.*, $21\times10^{-24}$ cm². From these measurements it would appear that the free neutron-proton cross section commonly accepted for theoretical calculations; *viz.*, $14\times10^{-24}$ cm² should be revised upward. The comparison measurements with cadmium absorption neutrons agreed well with values obtained by several other investigators using different methods for neutron detection, and the general results show that the method of working inside a collimating enclosure in the immediate vicinity of the cyclotron operates satisfactorily.

## INTRODUCTION

THE need for accurate investigation of the interaction of neutrons having well-defined energies in the low energy region (less than 1000 ev) has long been recognized. The resonance capture by certain elements of neutrons which have the proper energies provides a method for such energy selection through the use of these elements both as selective detectors and selective filters. The experiments described in this paper utilize this method together with the high intensities available from the cyclotron to obtain, in effect, a parallel beam of essentially "monochromatic" neutrons.

In a study of nuclear interactions involving these slow neutrons it becomes important for many considerations to distinguish between the various regions of the neutron energy spectrum. Recent experiments[1,2] have indicated the importance of investigations for neutron energies which are well above the thermal region and free from the uncertain effects of molecular interactions. This is particularly true for such cases as the neutron-proton and neutron-deuteron interactions. Theoretically, the results of such measurements should be much simpler to interpret, especially when the neutrons have a well-defined narrow energy range.

The selective resonance capture of neutrons in well-defined regions of the energy spectrum by various elements has been studied by many investigators.[3–8] Experiments with the cadmium mechanical velocity selector[9] showed that the neutrons emerging from paraffin, and which were strongly absorbed by cadmium, largely possessed thermal velocities and had a velocity distribution approximately Maxwellian in form, with a maximum at about 0.03 ev. The strong capture by elements such as rhodium, silver, indium, iodine, bromine and others, was shown by super-

* Publication assisted by the Ernest Kempton Adams Fund for Physical Research of Columbia University.
** Now at the College of the City of New York.
[1] H. G. Beyer and M. D. Whitaker, Phys. Rev. **57**, 976 (1940).
[2] F. Rasetti, Phys. Rev. **58**, 321 (1940).
[3] L. Szilard, Nature **136**, 950 (1935).
[4] E. Amaldi and E. Fermi, Phys. Rev. **50**, 899 (1936).
[5] P. B. Moon and J. R. Tillman, Proc. Roy. Soc. **153**, 476 (1936).
[6] H. H. Goldsmith and F. Rasetti, Phys. Rev. **50**, 328 (1936).
[7] Manley, Goldsmith and Schwinger, Phys. Rev. **55**, 39 (1939).
[8] Hornbostel, Goldsmith and Manley, Phys. Rev. **58**, 18 (1940).
[9] Dunning, Pegram, Mitchell, Fink and Segrè, Phys. Rev. **48**, 704 (1935).

position experiments to occur selectively for neutrons of particular velocities which differed for the various elements. The theoretical deduction and experimental proof that the strong neutron absorption in certain light elements, such as boron, varied inversely with the neutron velocity, provided a method for estimating approximately the velocity and thus the energy of these resonance neutron groups.

The process of selective absorption or resonance capture of certain neutrons by certain elements is accounted for in terms of a resonance phenomenon[10,11] of the neutrons associated with an energy level of the compound nucleus formed by the capture of the neutron by the nucleus. When the energy of the neutron is nearly that of one of these resonance levels, there is a large probability of capture generally followed by the emission of radiation which leaves the neutron bound in the nucleus. The energy width of the resonance capture level is related to the probability of re-emission of a neutron, and the probability of the emission of radiation or other particles.

While more exact measurements of the spectral position of such resonance levels should be carried out with more refined methods of neutron spectroscopy as they are being developed, the boron absorption method together with experiments on the self-absorption of neutrons in the same element has now yielded sufficient information to give at least a rough estimate of the position, width and height of the more prominent levels in the few nuclei thus far studied. The neutron velocity selection obtained by the modulated beam technique[12,13] has verified these results for cadmium and rhodium, and further development of this and other neutron spectroscopy methods will undoubtedly reveal more information.

The experiments described in this paper involve measurements made with the cadmium absorption neutrons, and the resonance neutrons of indium and iodine. As indicated above, the mechanical velocity selector showed that most of the cadmium absorption neutrons have energies corresponding to thermal velocities, although the cut-off for cadmium is beyond this energy at about 0.2 ev.[13] Indium shows a pronounced selective capture for neutrons characterized by having a relatively sharply defined energy in the region of 0.9 ev.[8] Another region of the neutron spectrum is that associated with the resonance capture in iodine, although here it seems likely that the energy (25–100 ev) is distributed among several levels.[14,15]

There are several factors associated with the indium-resonance neutrons which make them particularly desirable for interaction experiments. The energy of these neutrons is sufficiently beyond the thermal energy region to minimize the uncertain effects inherent in thermal neutron interactions, and yet the energy is sufficiently near the thermal region so that there is little extrapolation of the $1/v$ law for boron, thus allowing the energy to be determined with a fair degree of accuracy. The absorption of indium-resonance neutrons in boron exhibits a well-defined exponential decrease with thickness which strongly indicates that only one level or one narrowly defined region of the energy spectrum is responsible for most of the activation when thin samples are used. Furthermore the data from self-absorption experiments are consistent with a sharp narrow line (less than 0.1 ev wide) with a very high cross section[8] (approximately $20{,}000\times10^{-24}$ cm$^2$) at resonance, so that these neutrons are ideally suited for monochromatic beam measurements. Indium is also readily malleable and available in thin sheets—a convenience when the experimental arrangement is considered.

The interaction of slow neutrons with atomic nuclei can be appreciably influenced by interference effects when the neutrons have such energies that their de Broglie wave-lengths are of the order of magnitude of the interatomic spacing, as reported recently.[1,2] Thus thermal neutrons with a most probable wave-length of 1.7 angstrom units exhibit interference effects which in several cases should be absent when the measurements are repeated with indium-resonance neutrons of higher energy and shorter wave-length of approximately 0.3 angstrom unit.

[10] N. Bohr, Nature **137**, 344 (1936).
[11] G. Breit and E. Wigner, Phys. Rev. **49**, 519 (1936).
[12] L. W. Alvarez, Phys. Rev. **54**, 609 (1938).
[13] C. P. Baker and R. F. Bacher, Phys. Rev. **57**, 351 (1940).
[14] H. A. Bethe, Rev. Mod. Phys. **9**, 144 (1937).
[15] J. Hornbostel and F. A. Valente, Phys. Rev. **55**, 108 (1939).

In the case of compounds containing hydrogen the interaction of neutron and proton depends upon the relative values of the neutron energy and the energy of the lowest vibrational level of the hydrogen compound molecule.[16] Calculations indicate that these effects of molecular binding on the free neutron-proton interaction should be very small for neutrons of about 1-ev energy, so that indium-resonance neutrons with energy of about 0.9 ev should show very small effects due to molecular binding. However, in order to eliminate completely any such slight residual effects, measurements can be repeated with iodine-resonance neutrons having energies definitely beyond the binding range.

The desirability of investigating neutron interaction with neutrons having well-defined energies above the thermal region has resulted in several experiments using silver, rhodium, indium and iodine resonance neutrons for measuring the neutron-proton cross section.[17–19] Due to the low intensity of resonance neutrons obtainable with the natural radioactive sources used in these experiments, the results of some of these measurements are necessarily associated with poor geometrical arrangements and low statistical accuracy.

In the experiments described in this paper the cyclotron was used as a source of neutrons and the intensities available permitted measurements with large intensities as well as good geometry. The experimental work consisted of several rather separate parts; (1) Cross-section measurements of selected elements for indium-resonance neutrons; (2) investigation of interference effects; (3) measurement of the neutron-proton and neutron-deuteron interactions for indium-resonance neutrons and check measurements with thermal neutrons; (4) measurement of the neutron-proton interaction for iodine-resonance neutrons.

## Apparatus

In carrying out any transmission experiments with a beam of neutrons it is extremely important that good geometrical conditions prevail. Experiments under other conditions employing non-parallel neutron beams with both source and detector close to the sample have been shown to be unreliable, especially for samples containing hydrogen. The uncertain angular distribution of neutrons, together with large corrections for multiple scattering, slowing down processes, back scattering and obliquity make such experiments difficult to interpret. The design of the collimating device used in these experiments was such as to make errors introduced by geometrical factors almost negligible.

### Indium neutron collimator

Figure 1 shows the neutron collimator consisting of a boron-cadmium-indium lined enclosure with diaphragms located so that the incident and scattered portions of the beam are accurately defined. The double lines indicate cadmium sheet of 0.05 cm (43 mg/cm²) and the triple lines represent 0.0013 cm (9 mg/cm²) of indium between two sheets of cadmium. The housing surrounding the detector is of indium and cadmium, and serves to limit the "angle of vision" of the detector to the actual effective neutron beam. The monitor is so located that it "sees" only the incident beam and does not record any appreciable back scattering. Both detector and monitor are backed by 0.2 cm thickness of cadmium and 0.025 cm thickness of indium, and their front faces are covered with 0.15 cm of cadmium to exclude any activation due to residual thermal neutrons in the beam. The paraffin block serves to slow down the fast neutrons produced by the proton-beryllium reaction in the cyclotron and cadmium covers the front window to exclude thermal neutrons. Investigation showed that a thin paraffin layer of 1 to 2 cm thickness gave the maximum yield of slow neutrons under the conditions of the experiment. For the final neutron-proton measurements the cross section of the beam was divided into four quadrants (shown in dashed outline) by means of cadmium-indium partitions, so that the geometrical arrangement was materially improved. Actually the same measurements of the proton cross section were made with and without this cross collimation.

[16] E. Fermi, Ricerca Scient. **7**, 13 (1936).
[17] Cohen, Goldsmith and Schwinger, Phys. Rev. **55**, 106 (1939).
[18] Cohen, Goldsmith and Hornbostel, Phys. Rev. **57**, 352 (1940).
[19] L. Simons, Phys. Rev. **55**, 792 (1939).

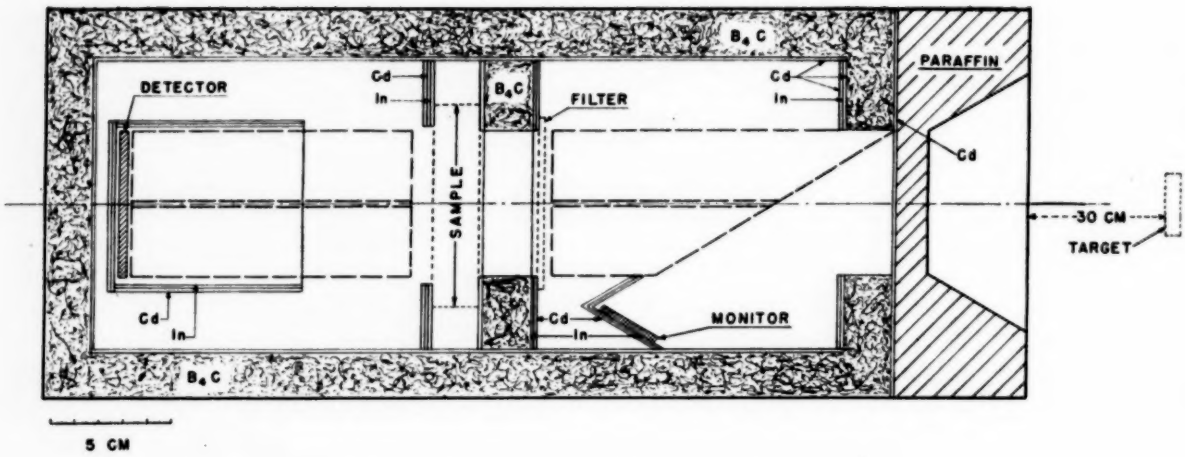


FIG. 1. Arrangement of indium resonance neutron collimator for transmission measurements.

**Detectors, monitors and selective filters**

It is essential in precision experiments of this kind, that the detector and monitor have "parallel" characteristics, and that both "see" only neutrons from the same effective source. The detectors and monitors used consisted of thin indium foil (27 mg/cm²) mounted on 0.013 cm thick sheet nickel holders, the detectors being circular of 6 cm diameter and monitors 2×4 cm. With such thin indium most of the induced activity is due to those neutrons near resonance where the cross section is a maximum. The nickel holders showed no observable activity for any of the radiation conditions encountered during the experiments. The selective filter employed to define further the neutron beam consisted of 33 mg/cm² of indium foil mounted on 0.013 cm thick aluminum sheet. This thickness reduced the open beam intensity by some 35 percent and represented a compromise which in effect absorbed only the "center" of the absorption line, thus removing a good fraction of the resonance neutrons from the beam without absorbing the "tails" of the line appreciably or the nonresonance neutrons comprising the background of the beam.

**Thermal neutron technique**

The same collimator was also used for making transmission measurements with thermal neutrons. For these experiments much thicker indium detectors and monitors were used and their faces covered with thick indium foil to minimize resonance activation. The front window of the collimator was covered with thick indium instead of the cadmium and the selective filter was a sheet of cadmium 43 mg/cm² (0.05 cm) thick. The same cross collimation was used.

**Iodine neutron technique**

In adapting the collimator for iodine-resonance neutron measurements the indium shielding was replaced with shield of tightly packed lead iodide. However, because of the much smaller capture cross section of the boron shielding for the higher energy neutrons, some fast neutrons could reach the detector from all directions, and activate the higher energy iodine levels appreciably. To make the boron and iodine more effective it was found necessary to shield the entire collimator by enclosing it in a paraffin house with walls some 20 cm thick. With this arrangement the neutrons exterior to the collimator were either removed or slowed down so effectively that the boron again showed a large capture cross section. The iodine filter finally adopted consisted of approximately 200 mg/cm² of iodine in the form of fused lead iodide deposited on 0.013 cm thick nickel sheet and reduced the open beam intensity by some 30 percent. Detectors and monitors were prepared in the same way by fusing lead iodide on the nickel. Four different detectors were used interchangeably, their thickness varying from 60 to 120 mg/cm². No cross collimation was used for the iodine measurements.

### Measuring system

The measuring system for following all the detector and monitor activities consisted of an ionization chamber connected to an Edelman string electrometer. The chamber with its 5-mil duralumin window was filled with Freon (difluorodichloromethane) to a gauge pressure of 60 lb./in.$^2$, and completely shielded with 3 cm of lead. With this arrangement the natural leak or background for the entire system was such that the ratio of time of drift due to natural leakage, to the time of drift resulting from the beta-radiation of a 100-mg standard of uranium oxide (wrapped in 1-mil aluminum foil) was better than 50 to 1.

### Samples

In most cases the samples used for neutron interaction measurements consisted of the particular elements of carefully determined purity and were of such thickness that 30 to 40 percent of the resonance neutrons traversing the sample were removed from the detected beam. With such transmissions the effect of double scattering was very small. For the measurements of the neutron-proton cross section, a carefully prepared sample of cetane ($C_{16}H_{34}$) was further purified by recrystallizing, melting, drying and filtering, and used in accurately machined, chromium-plated, thin brass cells with glass windows. Cetane was chosen because it is a paraffin which can be readily obtained in very pure form.

## Procedure

In using the resonance filter method for transmission measurements, the activities of detector (and monitor) had to be measured for each of the four conditions: (1) open beam; (2) filter in the beam; (3) sample in the beam; (4) both sample and filter in the beam. For a constant source of neutrons, the difference between (1) and (2) is proportional to the number of resonance neutrons passing down the beam; and the difference between (3) and (4) is proportional to the number of resonance neutrons passing through the sample without being scattered out of the beam. The transmission, $P$, is calculated from the relation

$$P=[(3)-(4)]/[(1)-(2)]$$

and the cross section found from the formula

$$P=e^{-\sigma N x}$$

where $\sigma$ is the total cross section (scattering plus capture), $N$ is the number of nuclei per cm$^3$, and $x$ the thickness in cm.

Since the output of the cyclotron during successive runs was not always the same, each detector activity was normalized to its respective monitor activity in terms of the uranium standard, so that any transmission value had to be found as the quotient of two quantities each of which was itself the difference of two quotients. Fifteen-minute radiation intervals generally gave sufficient activation of the 54-minute indium period so that detector activities were some thirty times the electrometer background, and monitor activities forty times this background.

Insofar as the measuring system was involved, any normalized detector activity could readily be determined with a precision measure of less than one percent with the usual nine readings to check detector and monitor activities. Over a long period it was found that repeated measurements of such normalized detector activity would never fluctuate by more than several times this precision measure, due to factors beyond reasonable control at the time. For example, complete data taken with one detector and its monitor over a period of several months showed that readings did not fluctuate more than a few percent and that the averaged values had a precision of 0.5 percent. During this interval the collimator and its paraffin front were separately removed and replaced numerous times. These results are of further interest in that they indicate the feasibility of working inside a collimating enclosure located in the immediate vicinity of the cyclotron. Generally the transmission could be readily measured with a precision appreciably better than 2 percent, so that cross section results are considered known to better than 5 percent. Better precision could be obtained when required by increasing the number of observations.

### Corrections

Because of the good geometry of the collimated beam, the corrections of the observed transmission were small. Obliquity corrections were so small ($<0.25$ percent) that they were neglected.

However, all observed transmissions were corrected slightly to account for the increased detector activity caused by the neutrons which, although scattered by the sample, did reach the detector. It was assumed, except for the proton measurements, that this scattering was spherical and that all neutrons scattered into the detector were still in the resonance region, thus resulting in the maximum possible geometrical correction which could be applied, since some of the neutrons scattered into the detector will have lost enough energy to reduce their probability of detection. For a transmission of 60 percent this correction amounted to about 0.5 percent with the cross collimated beam and about 3 percent for the earlier beam arrangement.

## Results

In Table I are given the results of measurements of the total cross sections of various elements for indium-resonance neutrons as well as several thermal neutron values. For further comparison the other corresponding thermal neutron cross sections have been included with appropriate references. In the cases of D, C, Fe, Ni, Cu, Pb, and Bi the same specimens were available for both sets of measurements, so that the results should be directly comparable. The scattering cross sections for thermal neutrons shown in the last column are those given by Goldhaber and Briggs.[20]

### Interference effects

A brief investigation of the interference effects mentioned previously was made by measuring the cross sections of several compounds in different crystalline states. Table II shows the results of measurements on single crystal quartz and finely divided sand for both indium-resonance and thermal neutrons. The value shown for sand with thermal neutrons was taken from the work of Beyer and Whitaker,[1] and is the result for the same sand as that for which the indium-resonance measurement was made.

Table I. *Cross sections of elements* $\times 10^{24}$ *cm*$^{-2}$.

| Element and Form | $\sigma$ for In Neutrons $E \approx 0.9$ ev | Thermal Neutrons $E \approx 0.03$ ev Total | Scat |
|---|---|---|---|
| H Cetane | 21.0±1.0 | 49.0 | |
| D $D_2O$ | 3.3 | 5.7 | |
| C Graphite | 4.9±0.2 | 4.9 | 4.8 |
| Al Metal | 1.5±0.1 | 1.5[1] | 1.6 |
| Fe Armco | 11.1±0.3 | 12.0[2] | 10.3 |
| Ni Rolled | 16.1±0.8 | 19.8[2] | 12.4 |
| Cu Rolled | 8.3±0.3 | 10.5[2] | 8.6 |
| Zn Metal | 4.2±0.2 | 4.5[2] | 5.2 |
| Sn Metal | 5.7±0.3 | | 4.9 |
| Pb Metal | 9.6±0.8 | 12.5[2] | 12.9 |
| Bi Metal | 8.7±0.5 | 8.9[2] | 8.9 |

[1] Dunning, Pegram, Fink and Mitchell, Phys. Rev. **48**, 265 (1935).
[2] H. G. Beyer and M. D. Whitaker, Phys. Rev. **57**, 976 (1940).

[20] M. Goldhaber and G. H. Briggs, Proc. Roy. Soc. **A162**, 127 (1938).

Table II. *Cross sections* $\times 10^{24}$ *cm*$^{-2}$.

| | In-Resonance Neutrons | Thermal Neutrons |
|---|---|---|
| Quartz Crystal (4.5 g/cm$^3$) | 7.5±0.5 | 4.3±0.3 |
| $SiO_2$ sand (3.3 g/cm$^3$) | 8.8±0.8 | 8.8±1.0 |

Measurements were also made with indium-resonance neutrons to determine whether there would be a change in the transmission for a physical mixture of the constituents of an alloy and the alloy itself. In the case of permalloy it was found that there was no difference in the transmission (within the precision of measurements) of a given thickness of Permalloy and an equivalent thickness of its nickel and iron components.

### Neutron-proton and deuteron measurements

Measurements of the neutron-proton cross section were made with a carefully prepared sample of cetane, $C_{16}H_{34}$, a standard hydrocarbon of known composition. The results for three thicknesses of cetane are shown by the logarithmic plot in Fig. 2 with the calculated precision of each point indicated. The two plots for indium-resonance neutrons are those corresponding to (*a*) transmission corrected for spherical scattering, (*b*) corrected for total forward scattering, assuming in both cases that all scattered neutrons reaching the detector remain within the energy region. Correction (*b*) represents the maximum possible geometrical correction which could be applied since some of the neutrons scattered into the detector will have lost enough energy to eliminate their detection. For these data the corresponding corrected neutron-proton cross sections for indium-resonance neutrons are (*a*) 20.3 and (*b*) $21.6 \times 10^{-24}$ cm$^2$, with the value $4.9 \times 10^{-24}$ cm$^2$ previously determined for the cross section of carbon. A more probable value would be between these two extremes, and for

the purpose of this paper it is given as $21\pm1 \times10^{-24}$ cm$^2$.

In order to verify the entire method of experiment, measurements were also made with the same cetane for thermal neutrons absorbed in cadmium. Thick indium detectors covered with indium to minimize resonance activation were used. The plot in Fig. 2 also shows the transmission for thermal neutrons absorbed in cadmium, corrected for spherical scattering and gives a value for the neutron-proton cross section of $49.0\times10^{-24}$ cm$^2$. If there is a small amount of forward scattering this value would be increased slightly. This result is in good agreement with the values previously obtained with the boron or lithium $1/v$ law detectors and ion-chamber-linear amplifier systems and shows that this method operates satisfactorily.

The results for the deuteron cross section were obtained from transmission measurements on two thicknesses of deuterium oxide, and the logarithmic plot in Fig. 3 gives these data corrected for spherical scattering both for indium-resonance neutrons and thermal neutrons. The cross section for indium-resonance neutrons is found to be $3.3\times10^{-24}$ cm$^2$, taking the cross section for oxygen to be $4\times10^{-24}$ cm$^2$.[21] The corresponding thermal neutron value from these data was found to be $5.7\times10^{-24}$ cm$^2$. The $D_2O$ used in these experiments was kindly supplied by Professor Urey and the original analysis indicated a purity of 99.8$^+$ percent, so the correction for presence of ordinary hydrogen should be small.

**Iodine measurements**

The measurements with iodine-resonance neutrons were made with the same cetane specimens used earlier and Fig. 4 gives the logarithmic plot of the transmission corrected for spherical scattering. For comparison the corresponding transmission for indium neutrons (found before cross collimation was added) is shown by the second set of points, indicating that there is no appreciable difference between the two values. From this plot the iodine-resonance neutron-proton cross section becomes $20\times10^{-24}$ cm$^2$ (with the value of $4.9\times10^{-24}$ cm$^2$ previously determined for the cross section of carbon for these same neutrons). As mentioned earlier, these iodine neutron readings were taken without the cross collimation used for the final indium neutron experiments, so that the absolute values of the neutron-proton cross section for iodine neutrons could not be determined with the same accuracy. The experiment does show that there is no experimentally observable difference between the neutron-proton cross sections for neutrons of approximately 1-ev energy and those with an energy of the order of 25 to 100 ev.

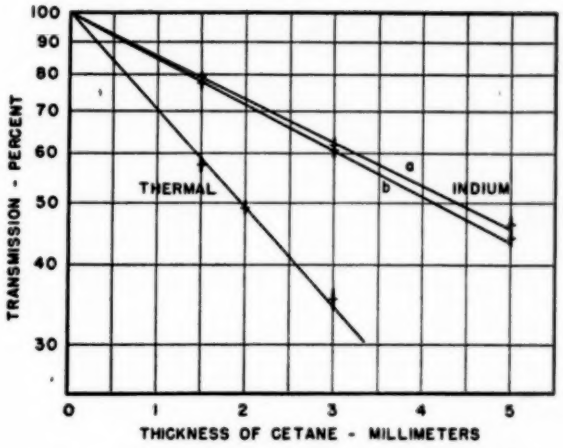


FIG. 2. Transmission of slow neutrons in cetane.

## DISCUSSION

The theory of scattering and capture interaction of slow neutrons with atomic nuclei has been developed by Breit and Wigner.[10] If it is assumed that there is only one nuclear resonance level involved; and that the neutron width $\Gamma_n$ is small compared with the sum of all the other partial widths $\Gamma$, (i.e., if the probability of re-emission of a neutron is small compared with that for radiation) then the expressions for consideration are

$$\sigma_{\text{capture}}=\frac{h^2}{8\pi M(EE_r)^{\frac{1}{2}}}\frac{\Gamma_n\Gamma}{(E-E_r)^2+\frac{1}{4}\Gamma^2},$$

$$\sigma_{\text{scattering}}=\frac{h^2}{8\pi ME_r}\frac{\Gamma_n^2}{(E-E_r)^2+\frac{1}{4}\Gamma^2}.$$

Here $E$ denotes the kinetic energy of the neutron, $M$ its mass, and $E_r$ the resonance energy. The energy widths $\Gamma$ and $\Gamma_n$ represent the energy

[21] H. Carroll and J. R. Dunning, Phys. Rev. **54**, 541 (1938).

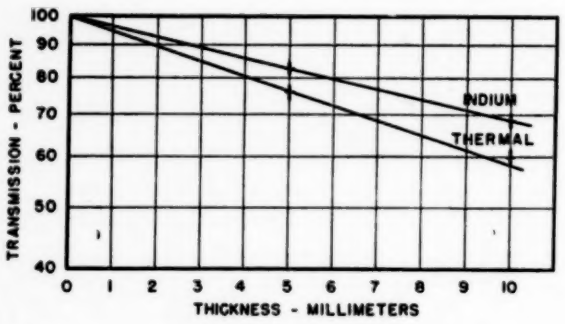


FIG. 3. Transmission of slow neutrons in deuterium oxide ($D_2O$).

range over which the cross section is greater than half of its maximum value. In the case of the capture cross section there is not only the resonance factor $(E-E_r)^2$ but also the factor $E^{-\frac{1}{2}}$ representing the $1/v$ variation of the absorption cross section. For $E$ very small compared with the resonance energy and the total width $\Gamma$, this $1/v$ factor will be dominant.

An inspection of the cross sections shown in Table I indicates that there is in general a decrease in the total (scattering plus capture) interaction for the indium-resonance neutrons as compared with the thermal neutron value. Such a difference is consistent with the lower probability of nuclear capture of the indium-resonance neutrons since the capture process is a more critical function of neutron energy than the scattering interaction due to the factor $E^{-\frac{1}{2}}$ mentioned above. A further comparison of these same indium-resonance values with the scattering results for thermal neutrons found by Goldhaber and Briggs does not show the same consistency, especially for the element Pb. However, in this case the total cross sections for both indium and thermal neutrons were measured on the same Pb sample, with the same order of precision, so that these two values are directly comparable. Even if there should be no contribution of the capture process to the total cross section of Pb for thermal neutrons, it does not seem likely that the scattering interaction should vary as rapidly with energy as would be required by the scattering data and the data for the indium-resonance neutrons. As a general rule, the scattering cross section for slow neutrons is considered independent of neutron energy, since the neutron width $\Gamma_n$ is very small compared with $\Gamma$.

The data in Table I would also indicate that for the elements C, Al, Fe and Bi, the interaction of neutron and nucleus in this energy region is almost entirely a scattering process. In the case of carbon this is further verified by the data obtained for iodine-resonance neutrons which is identical with the data found for the other two neutron energies.

The measurements on single crystal and polycrystalline quartz are only of interest in that they agree with the results of a similar experiment performed by Whitaker, Bright and Murphy,[22] using a different method of neutron detection.

The neutron-proton cross section found for indium-resonance neutrons agrees well with the value of $20\pm2\times10^{-24}$ cm$^2$ found by Cohen, Goldsmith and Schwinger[17,18] for the resonance neutrons of rhodium, indium and silver. It is considerably higher than the value of 10 to $12\times10^{-24}$ cm$^2$ originally obtained by Amaldi and Fermi.[23] In the case of the neutron-proton value for the cadmium absorption neutrons the value of $49\times10^{-24}$ cm$^2$ is in very good agreement with recent determinations; *viz.*, 50.0,[24] 49.0,[25] and 47.5[26] where different methods of neutron

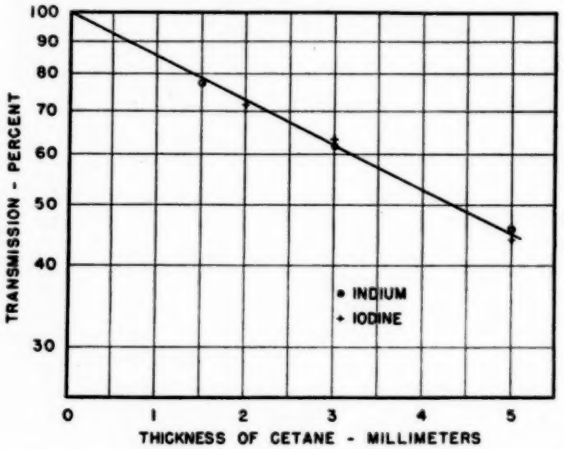


FIG. 4. Transmission of slow neutrons in cetane ($C_{16}H_{34}$).

[22] Whitaker, Bright and Murphy, Phys. Rev. **57**, 551 (1940).
[23] E. Amaldi and E. Fermi, Ricerca Scient. **7**, 310 (1936).
[24] H. Carroll and J. R. Dunning, Phys. Rev. **54**, 541 (1938).
[25] Frisch, v. Halban, and Koch, Kgl. Danske Vid. Sels. Math.-fys. Medd. **15**, 10 (1938).
[26] M. Goldhaber and G. H. Briggs, Proc. Roy. Soc. **A162**, 127 (1937).

detection were used, and shows that the method of working inside such a collimating enclosure with the cyclotron yields results consistent with other techniques.

A consideration of the results obtained for the deuteron interaction indicates that the cadmium absorption value is in good agreement with the value of $5.7\times10^{-24}$ cm² obtained by Carroll and Dunning.[27] The indium-resonance value for the deuteron interaction was found to be $3.3\times10^{-24}$ cm², and it is of interest to investigate the effect of molecular binding on this interaction. If the capture contribution in this interaction be assumed very small, the scattering cross section would vary as the square of the reduced mass of the system, associating the indium neutron value with the free deuteron interaction, and the thermal neutron result with the bound deuteron cross section. This molecular binding effect would reduce the thermal neutron value of $5.7\times10^{-24}$ cm² to a minimum of $2.8\times10^{-24}$ cm², which is in fair agreement with the experimental value of $3.3\times10^{-24}$ cm², especially since this correction assumes infinite molecular binding for the deuteron. The theoretical calculations of Motz and Schwinger[28] give appreciably higher values for the deuteron-neutron interaction but their results are subject to approximations which would be expected to give a higher value.

The results for the neutron-proton interaction for iodine-resonance neutrons are of particular interest, since the minimum value of the cross section was found to be $20\times10^{-24}$ cm². This is considerably higher than the value of $14.8\times10^{-24}$ cm² recently reported by Simons[19] for the same energy neutrons but with poor geometry. The author also reports the same value for this cross section when the measurements were repeated with silver resonance neutrons (energy 3 ev) and this result is at variance with the value of $20\times10^{-24}$ cm² reported by Cohen, Goldsmith and Hornbostel[18] for these same neutrons. Since the data taken in these experiments on the cetane samples for cadmium and indium neutrons agree well with the results found by several other investigators, the values of the neutron-proton cross section for the three different neutron energy groups should be directly comparable. It is difficult to account for the value of $14.4\times10^{-24}$ cm² for the neutron-proton interaction recently reported by Amaldi, Bocciarelli and Trabacchi[29] using rhodium neutrons. However, the rhodium filter used was exceedingly thick and may partially account for such a low value.

The effects of molecular binding on the neutron-proton interaction have been extensively investigated and lead to the conclusion that these effects should already be very small for neutrons of about 1-ev energy. This prediction is verified by the results of these experiments in view of the agreement between the iodine and indium resonance neutron interactions for the proton. If this is the case then it appears that the free neutron-proton cross section commonly accepted for theoretical calculations; *viz.*, $14\times10^{-24}$ cm² should be revised upward to approximately $21\pm1\times10^{-24}$ cm².

### Acknowledgments

The author wishes to express his appreciation for the helpful guidance of Professor J. R. Dunning at whose suggestion this problem was undertaken. The cooperation of the members of the Cyclotron Staff is thankfully acknowledged, particularly the unfailing efforts of Mr. H. Glassford whose skillful operation of the cyclotron over extended periods made possible the completion of this work within a reasonable time, and the timely and able assistance of Mr. E. P. Blizard in conducting the iodine neutron experiments. The aid of the Research Corporation is gratefully acknowledged and particular thanks are extended to the Indium Corporation of America for the loan of several ounces of indium. Acknowledgment is made to the U. S. Work Projects Administration of New York City for assistance rendered under project number 24.

[27] H. Carroll and J. R. Dunning (unpublished).
[28] L. Motz and J. Schwinger, Phys. Rev. **58**, 26 (1940).
[29] Amaldi, Bocciarelli and Trabacchi, Ricerca Scient. **11**, 121 (1940).

# A Concentration Method for Certain Radioactive Metals*

JOSEPH STEIGMAN**
*Pupin Physics Laboratories, Columbia University, New York, New York*
(Received January 20, 1941)

An extension of the Szilard-Chalmers concentration technique to radioactive metals is discussed. The principle involved is the choice of certain metal complex compounds which are highly stable and which have also been resolved into stable optical isomers. The technique is applied to Co, Ir, Rh and Pt complex salts, with resulting high concentration ratios.

FROM the chemical point of view, there are, in general, two types of nuclear transformations: those in which a change in atomic number accompanies the reaction; e.g.,

$$_{30}Zn^{64}+{}_0n^1\rightarrow{}_{29}Cu^{64}+{}_1H^1$$

and those in which a radioactive isotope of the bombarded element is formed as in the case of simple neutron capture:

$$_{53}I^{127}+{}_0n^1\rightarrow{}_{53}I^{128}+\gamma.$$

The separation of radioactive from nonradioactive species is comparatively simple for the first type. It consists merely of adding a small amount of "carrier" inactive material (such as $CuSO_4$) to the system, and performing routine chemical separations. The second case, however, is far more difficult, because of the identity of ordinary properties common to both the radioactive element and the inactive isotope from which it is derived. In this connection, Szilard and Chalmers[1] have established a general principle to be applied to such concentration problems. When an atom captures a slow neutron and emits a gamma-ray, the energy of the recoil of the nucleus is in general much greater than that of any chemical bond. The chemical molecule is therefore decomposed, and the radioactive atom is usually ejected from its chemical binding as a "free" atom or ion. If the original chemical binding is of such a nature that little or no exchange will occur between the "free" radio-isotope and the chemically combined inactive material, a chemical separation of the two species will succeed in concentrating the radioactivity. In general, this means the choice of a so-called molecular or nonpolar type of binding in contradistinction to that of ionic compounds. For example, Szilard and Chalmers bombarded ethyl iodide with slow neutrons, added a trace of iodine and separated the two. They found that most of the radioactivity was concentrated in the iodine. Potassium iodate has been used in place of ethyl iodide for a similar purpose, and this technique has been extended to all the halogens, as well as arsenic and a number of other nonmetals.

In the case of metals, however, no general criterion for the choice of suitable stable compounds has as yet been put forth, and no general success has been achieved in concentrating radioactivity. It is, of course, obvious that a "molecular" type of binding is necessary; but the problem arises—how is such a binding to be recognized. There are a number of possible qualities which would indicate the existence of the desired bond type; i.e., one with weak external molecular fields of force. These qualities include volatility, low melting point, solubility in organic media. They are, in general, the properties of that group of substances known as metal-organic compounds; e.g., zinc dimethyl. Unfortunately, however, for a very large group of metallic elements in the periodic table, particularly those of the Bohr transition group, no metal-organic derivatives have as yet been synthesized, although numerous attempts have been made in the past 80 years. It is obvious, therefore, that for the present, at least, one must turn elsewhere for *general* types of suitable stable compounds with a *general* underlying criterion for concentrating radioactivity.

Examination of the chemistry of the metallic elements in the periodic table indicates that there is a large group of compounds common to

* Publication assisted by the Ernest Kempton Adams Fund for Physical Research of Columbia University.
** Now at the College of the City of New York.
[1] L. Szilard and T. Chalmers, Nature **134**, 462 (1934).

most of them. This is the so-called "complex" compound or "Werner complex" compound type, e.g., ammonia, ethylene diamine or oxalic acid, etc., complexes of the metals involved. These substances, in addition to being numerous, are also comparatively simple to prepare and to preserve. Now from among the numerous properties of these complexes, we shall select one, which we shall attempt to utilize as *one of a number of possible criteria* for radioactive concentration. It should be stated at this point that the particular criterion selected does not raise the immediate quantitative problem of strength of chemical binding. Rather, it raises the related question of the rate of exchange between the metal complex and the "free" metallic ion. The criterion involved postulates a very low or practically zero rate of exchange in the cases to be cited. . . . Werner[2] was able to resolve (i.e., separate) certain of these complex compounds into optical enantiomorphs, one of which rotated the plane of polarized light to the right, and the other equally to the left. Some of the compounds which were resolved preserved their optical rotatory power unchanged over long periods of time, whereas other racemized; i.e., lost their optical activity on standing. The following postulate is now advanced: If a complex compound has been separated into optical enantiomorphs, and if these enantiomorphs retain their optical rotatory power unchanged over a period of time, then no exchange exists between this complex compound and its "free" metallic ion. That is, the rate of such exchange is practically zero. The reasoning behind the postulate is the following: If there were exchange between the "free" metallic ion and the complex compound, the optical isomers of the latter *must* dissociate and recombine in regular equilibrium fashion. Now the probability of formation of a dextro-isomer on recombination is the same as that of a laevo-isomer. For example:

(1) laevo iridium triethylene diamine ion→iridium ion (inactive)+ethylene diamine

(2) iridium ion (inactive)+ethylene diamine ⇄dextro and laevo iridium triethylene diamine ion in equal quantity.

Such a process inevitably results in loss of optical activity (racemization). Hence, it is postulated, if no racemization is found to occur with a particular complex compound, then no exchange takes place between the complex and the "free" metallic ion. In addition, if the complex compound were irradiated, and the radioactive metal ejected as a "free" ion, a chemical separation would result in a concentration of radioactivity.

It must be emphasized at this point that the above criterion is not the *only* one possible, but is merely a general one which is advanced. Undoubtedly further studies of Werner complex compounds will bring to light other criteria at least equally wide in range of application. In addition, it must be stated that it is not necessary to separate a complex into optical isomers for concentrating radioactivity. If the chemical literature reports the existence of stable optical isomers of a particular compound, then the racemic form (i.e., the one obtained in ordinary laboratory synthesis) is suitable. In the experimental work to be described here, only racemic compounds were employed.

There are three main types of complex metal compounds which have been successfully resolved:[3]

1. The trioxalate complexes as, $K_3(Co(C_2O_4)_3)$.
2. The triethylene diamine complexes as $(Ir(NH_2CH_2CH_2NH_2)_3)Cl_3$.
3. The tri-dipyridyl complexes, as

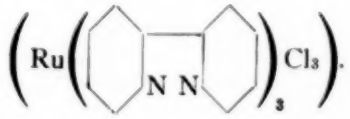


The metals whose resolved compounds belong to any or all of the three types include: Cr, Fe, Co, Al, Rh, Ir, Pt, Zn, Cd, Ni, Ru. The triethylene diamine complexes are the most stable of the three groups.

The following compounds have been prepared

[2] A. Werner, *New Ideas on Inorganic Chemistry* (Longmans, Green and Co., London, 1911).

[3] H. Emeleus and J. Anderson, *Modern Aspects of Inorganic Chemistry* (G. Routledge and Sons, Ltd., 1938), p. 98.

in order to test the postulate stated above:

(Ir (*en*)$_3$) (NO$_3$)$_3$,[4] *en*≡ethylene diamine,
(Pt (*en*)$_2$) (NO$_3$)$_2$,[5]
(Co (*en*)$_3$) (NO$_3$)$_3$,[6]
(Rh (*en*)$_3$) (NO$_3$)$_3$,[7]
(Ru (*dipy*)$_3$) Cl$_2$,[8] *dipy*≡dipyridyl.

It should be noted that the compound (Pt (*en*)$_2$) (NO$_3$)$_2$ has not itself been resolved. However, a substituted ethylene diamine platinum complex[9] has been successfully resolved. There is very little reason to expect any remarkable shift in bond strength between platinum and nitrogen because of the substitution.

## Experimental

Approximately one gram of each complex salt was prepared, except for the ruthenium compound. Only half a gram of the latter was synthesized. The salts were obtained originally as chlorides and all except the ruthenium compound were coverted to nitrates by the action of excess silver nitrate. The excess silver ion was removed by the addition of ammonium thiocyanate. The resulting solution had a volume of 15 cc. It should be pointed out that while the metal is present in the compound to but a small atomic percent, the metallic atom in question accounted for most of the effective neutron capture cross section for the compound. Furthermore, since these substances normally will be irradiated in water solution, the presence of hydrogen in the compounds is of advantage for slow-neutron irradiation.

The Ir, Co, Pt and Ru solutions were bombarded intermittently by slow neutrons in the Columbia cyclotron for approximately one month. The rhodium complex solution was irradiated for five minutes. The general technique of separation for the platinum metals consisted of the addition of 10–20 milligrams of "carrier" metallic chloride, followed by the addition of zinc dust and a little hydrochloric acid. The "free" metal ion was reduced to the metal, and filtered off with the excess zinc dust. In the case of iridium, and rhodium, the filtrate was treated with saturated KI solution to precipitate the complex iodide salt. The platinum filtrate was treated with alcoholic LiCl, which precipitated the complex chloride. Under these particular conditions, ammonium chloride did not precipitate. Ammonium thiocyanate was used to precipitate the complex salt from the ruthenium filtrate. The various precipitates were filtered off on a Büchner funnel, dried with alcohol and ether, and covered with Cellophane tape. The activities were then measured either with an ionization chamber—electrometer system (FP-54 circuit) or a Geiger-Müller counter. It should be noted that certain analytical difficulties (as the precipitation of ammonium chloroplatinate when chloroplatinic acid was added to the active solution) can be avoided, and in any case do not interfere with the reduction of the metallic ion to the metal.

The cobalt complex salt required a different approach inasmuch as the reduction of the ion to the metal is difficult to achieve. After preliminary experiments indicated that cobalt sulfide was so insoluble that the complex salt lost cobalt ion to sodium sulfide solution, the cobalt thiocyanate compound was employed. The active solution was treated with sufficient solid $NH_4CNS$ to make a 30-percent solution by weight, several drops of a 1 *M* cobalt nitrate solution were added, as well as an ether-amyl alcohol mixture. The system was transferred to a separatory funnel, and shaken. The aqueous lower layer was drawn off and treated with saturated KI solution. This precipitated (Co (*en*)$_3$) I$_3$. Hydrochloric acid was added to the ether layer and decomposed the ether-soluble cobalt-thiocyanate compound. The active cobalt was then extracted with water, the solution neutralized, and treated with sodium sulfide solution. The cobalt sulfide precipitate was filtered off, washed, and dried.

It must be admitted that the analytical procedure outlined above for cobalt is too complicated. In addition, it has the possible disadvantage of promoting exchange between free ion and complex during the course of separation. However, it should be looked upon as a make-shift separation made to establish the

[4] V. V. Lebedinski, Ann. Inst. Platine, No. 4, p. 235 (1926).
[5] S. M. Jorgensen, J. Prakt. Chim. **39**, 1.
[6] A. Werner, Ber. **45**, 125.
[7] A. Werner, Ber. **45**, 1231.
[8] F. H. Burstall, J. Chem. Soc. p. 173 (1936).
[9] W. Mills and T. Quibell, J. Chem. Soc. p. 839 (1935).

general principle outlined above, rather than as an adequate separation of cobalt-ion from the complex salt.

The experimental results are outlined in Table I. It should be noted that these ratios have not been "corrected." That is to say, they are ratios peculiar to the particular quantities of complex compound and "carrier" metal chloride used in these experiments. These ratios can be increased many-fold (a) by increasing the quantity of complex compound, and/or (b) reducing the quantity of "carrier" metal chloride used. In all these cases, therefore, the method is very successful in concentrating virtually all the radioactivity.

TABLE I. *Ratio of concentrate activity to activity of the complex salt.*

| Element | Rh | Ir | Pt | Co | Ru |
|---|---|---|---|---|---|
| Activity ratio | 150 | 56 | 44 | 10 | ?* |

* No activity detectable in either chemical fraction.

## CONCLUSION

The general principle therefore appears to be established that a metal complex compound whose optically active isomers do not racemize can be used to concentrate radioactivity produced by simple neutron capture. Several points should again be noted in this connection. It is not necessary to resolve such a compound into its enantiomorphs in order to concentrate the metallic radioactivity. The racemic compound will, of course, be suitable. Secondly, the above criterion is a sufficient one, but not a necessary one. Other criteria undoubtedly will serve as well. It may well be that even those complex compounds whose enantiomorphs racemize rapidly can still be used.

The support of the Research Corporation is gratefully acknowledged. The cooperation of the American Platinum Works of Newark, New Jersey, which supplied the iridium and ruthenium chlorides, is much appreciated.

---

MARCH 15, 1941 PHYSICAL REVIEW VOLUME 59

# The Absolute Number of Quanta from the Bombardment of Fluorine with Protons†

JAMES A. VAN ALLEN* AND NICHOLAS M. SMITH, JR.*
*Department of Terrestrial Magnetism, Carnegie Institution of Washington, Washington, D. C.*

(Received January 30, 1941)

From recent experiments it seems very probable that the 6.2-Mev quanta from the proton bombardment of fluorine are associated in one-to-one correspondence with the short range alpha-particles. This correspondence makes possible the establishment of the gamma-ray intensity by measuring the alpha-particle yield. With a specially designed variable pressure absorption-cell ionization-chamber to facilitate clear distinction between the short range alpha-particles and the scattered protons, the angular distribution and total yield of the alpha-particles at the lowest resonance (330 kv) have been determined. The determinations were based on plateaus appearing in curves of counting rate as a function of (1) cell pressure, (2) counter bias, and (3) bombarding voltage at angles of 60°, 90°, 120°, and 150° with respect to the proton beam. The results show that: (*a*) To within two percent the angular distribution of the alpha-particles is spherically symmetric; and (*b*) the yield over $4\pi$ steradians is $8.9\pm0.5\times10^4$ alpha-particles per microcoulomb of 360-kv protons bombarding a thick crystal of $CaF_2$. The absolute number of quanta from the reaction is presumably the same to the same accuracy. With both a heavily shielded counter and a similarly protected electroscope the ratio of the gamma-ray intensity at 1050 kv to that at 370 kv was found to be $42.0\pm0.8$. Thus the gamma-ray intensity at 1050-kv bombarding voltage is $3.7_4\pm0.2\times10^6$ quanta per microcoulomb of protons on $CaF_2$. The angular distribution of the gamma-radiation was found to be spherically symmetric to within the experimental error of five percent. Knowledge of the absolute intensity of the fluorine source greatly enhances its value in photo-nuclear and other experiments.

## INTRODUCTION

IN connection with experiments on photo-nuclear effects a source of high energy gamma-radiation of known quantum-intensity is needed; monochromatic radiation also is very desirable. The best such natural source is ThC″ ($E_\gamma=2.65$ Mev). Of the artificial sources which have been investigated the resonance reactions of protons

† Reported at November, 1940, meeting of American Physical Society, Chicago, Illinois.
* Carnegie Institution Fellow.

on fluorine ($E_\gamma = 6.2$ Mev) and protons on lithium ($E_\gamma = 17.5$ Mev) are the ones which yield gamma-rays best suited to quantitative measurements.

The mechanism of the fluorine reaction suggests a method of quantum calibration which is ideal in its simplicity and directness. There now exists strong evidence[1] to show that the disintegration proceeds as follows:

$$F^{19}+H^1 \rightarrow O^{16*}+He^4+Q_1, \qquad (a)$$

$$O^{16*} \rightarrow O^{16}+\gamma+Q_2, \qquad (b)$$

where $Q_1 = 1.79$ Mev and $Q_2 = 6.2$ Mev. The evidence consists of the facts (1) that the alpha-particle resonances occur within the experimental error at the same bombarding voltage as the gamma-ray resonances, (2) that the alpha-particle in (*a*) takes up the expected fraction of the energy of the incident proton while the gamma-ray has the same energy at all resonances investigated,[2] that is, that $Q_1$ and $Q_2$ are constants, and (3) that $Q_1+Q_2=Q_3$, where $Q_3$ (= 7.95 Mev) is the energy released in the production of long range alpha-particles:[3]

$$F^{19}+H^1 \rightarrow O^{16}+He^4+Q_3. \qquad (c)$$

The one-to-one correspondence[4] in the emission of an alpha-particle and a quantum according to (*a*) makes possible the establishment of the gamma-ray intensity by measuring the alpha-particle yield.

The angular distribution and absolute yield of these heavy particles have been measured; in view of the evidence outlined above, this yield is presumably equal to the quantum intensity of the gamma-radiation.

The 330-kv resonance was chosen for two reasons: (1) It is probable that no pairs are emitted at this resonance;[5] (2) it is possible only at this resonance for reasons stated below to detect the alpha-particles by range differentiation.

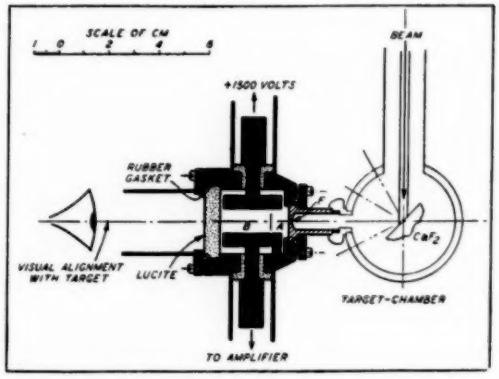


FIG. 1. The variable pressure absorption-ionization cell. The method of visual alignment is indicated in the drawing. (Details of beam collimation are given in Fig. 5.)

Once the absolute intensity at 330 kv is established, then a valid intensity comparison with the higher resonances can be made by a counter or ionization chamber, since the character of the radiation is the same.[2]

## EXPERIMENTAL

### The absorption cell

Even at 330 kv the difference between the ranges of the alpha-particles and the protons scattered elastically from the target is small and the scattered protons far exceed in number the disintegration particles. Under practical counting conditions the region in which the two types of particles can be clearly distinguished is less than one millimeter of range. Thus, a counting method of high resolution is required. For the final measurements a variable pressure absorption-ionization cell of the type used by Allison and associates[6] was designed so as to be well adapted to yield measurements (Fig. 1). It is to be noted that in this chamber the absorption cell and the ionization chamber operate at the

[1] W. B. McLean, R. A. Becker, W. A. Fowler and C. C. Lauritsen, Phys. Rev. **55**, 796 (1939); W. E. Burcham and C. L. Smith, Nature **143**, 795–796 (1939); W. E. Burcham and S. Devons, Proc. Roy. Soc. **A173**, 555–568 (1939).

[2] P. I. Dee, S. C. Curran and J. E. Strothers, Nature **143**, 759–760 (1939); and L. A. Delsasso, W. A. Fowler and C. C. Lauritsen, Phys. Rev. **51**, 527 (1937).

[3] M. C. Henderson, M. S. Livingston and E. O. Lawrence, Phys. Rev. **46**, 38–42 (1934).

[4] Above 0.68 Mev, Lauritsen and others have shown that another excited state of the oxygen nucleus is associated with a short range alpha-particle and can lose its energy by electron-pair emission according to $O^{16**} \rightarrow O^{16} + \pi + 5.9$ Mev. See W. A. Fowler and C. C. Lauritsen, Phys. Rev. **56**, 840–841 (1939).

[5] Private communication. Streib, Fowler and Lauritsen state that at this resonance their method of detecting nuclear pairs would have revealed as few pairs as one-half percent of the number of quanta observed.

[6] S. K. Allison, L. C. Miller, G. J. Perlow, L. S. Skaggs and N. M. Smith, Jr., Phys. Rev. **58**, 178 (1940); G. J. Perlow, Phys. Rev. **58**, 218–225 (1940); and L. C. Miller, Phys. Rev. **58**, 935–942 (1940). See H. Geiger, Zeits. f. Physik **8**, 45–57 (1921) for an early use of the usual form of absorption cell.

same pressure, which can be varied widely. In the ordinary case the pressure is varied in only the absorption cell and the ionization chamber works at atmospheric pressure. However, the two methods have similar characteristics[6] as long as the ionization chamber in the former case is deep, that is, as long as the particle is completely stopped by the air in the sensitive region. If the plates of the ionization chamber are perpendicular to the path of the particle, two disadvantages result: In order to have a deep chamber an inconveniently high sweeping voltage is required, and a metallic screen or foil is needed to separate the absorption region from the collection region. Screens reduce the effective aperture in an uncertain manner. Foils introduce undesirable stopping and, if quite thin, are subject to acoustical disturbances.

The use of plates parallel to the average path of the alpha-particles rather than perpendicular makes it possible to separately define the absorption region *A* and the ionization chamber *B* without the use of screens or foils. This is accomplished by the fact that the lines of force are perpendicular to the path of the particle and all the positive ionization in the region *A* is attracted to the grounded electrode, all in *B* to the grid electrode of the amplifier. Furthermore, one can make the sensitive region very deep—in this case 17 mm—increasing the useful pressure range of the instrument without requiring an unusually high voltage (1500 volts was used on the plates for the spacing of 8 mm). The range dispersion was made high by constructing the absorption region *A* only 7 mm deep. Thus a change of pressure of 10 cm of mercury in the cell corresponded to a change in stopping power of roughly 1 mm of normal air. This is indicated by the horizontal arrow in Fig. 2. This design reduces the instrumental straggling (and consequently increases the resolution) by affording complete electrical and acoustical shielding. The first stage of the amplifier was isolated mechanically from the cell.

The aperture *F* was the only one which limited the solid angle subtended from any point of the effective target. This arrangement simplified the calculation of the total yield. The plates of the cell were sufficiently far apart (8 mm) so that alpha-particles leaving anywhere from a target area 9 mm in diameter would enter the cell and be detected. The maximum size of the beam at the target was a circle of only 4 mm diameter. In addition to this precaution the "Lucite" window on the back of the cell permitted its accurate alignment by viewing through the window and through the aperture *F* the blue fluorescent spot produced by the proton beam on the calcium fluoride crystal used as a target. The cell was adjusted until the light from the average position of the fluorescence passed through the center of the chamber and was safely distant from the collection plates. In this manner it was assured that all particles coming from the target and penetrating the window *F* would be counted. A brass shielding cap was put over the "Lucite" window while it was not being used to view the target-cell alignment.

**Beam collimation and measurement**

The beam of protons was collimated by two holes (*A* and *B* in Fig. 5) 0.32 cm in diameter and 22 cm apart. The target was located 16 cm below *B*. Therefore, the maximum possible excursion of the beam at the target was within a circle of 4 mm diameter. Measurements of the carbonized spot on the surface of the target after bombardment proved this to be the case. The electrode *C* was maintained at −45 volts to prevent the loss of secondary electrons from the target chamber. The electrode *D* was grounded to prevent leakage from *C* to the target. No change in the beam current reading (sensitivity one percent) could be observed for a variation of the potential of *C* from 0.0 to −135 volts. No leakage in the order of 0.001 microampere could be observed between *D* and the target-chamber when 135 volts were applied. Secondary electron-current to the grounded window frame *F* was not measurable and was therefore less than 0.1 percent. A slight charging up of the target-face was probably helpful in preventing secondary electrons from leaving the target. The current to the target was read at 10-second intervals during the runs with a Sensitive Research model 55 microammeter and the average taken. This meter was calibrated in two ways by comparing it (1) with a Leeds and Northrup standard resistor and Weston labora-

tory standard voltmeter and (2) with a previously unused Sensitive Research model J–W microammeter. The two methods gave the same result to within less than one-half percent. The bombarding current was held low to values of the order of 3 microamperes to prevent superposition of the pulses caused by the scattered protons. All runs during which the current fluctuated seriously were discarded.

It is unlikely that the average value of the current over a set of runs was in error by more than one percent. The magnetically separated proton beam was used in all measurements. The fact that no measurable current was ever found between the mass-one and mass-two spots made it certain that no appreciable number of molecular ions of partial energy was present in the mass-one spot. The current in the single mass spot usually constituted about 80 percent of the total beam down the accelerating tube.

**Thin-window calibration**

The aperture $F$ was a single hole of about 0.05 cm diameter made vacuum tight by a collodion film (pharmacist's "Newskin") of 1 to 2 mm air equivalent. The film was prepared in the usual way by spreading of the collodion solution on water and sealed to the window frame with "Apiezon W." Examination of the films with a low power microscope usually showed the presence of a slight amount of dust. The presence of these foreign particles had the effect of decreasing the effective aperture of the window. Therefore, the transmission factor of the film was always experimentally determined.

A thin polonium source was deposited on a silver button from a mother solution of RaD, E, F prepared by Dr. L. R. Hafstad, and was so arranged as to permit its accurate replacement with respect to the window holder. The number of alpha-particles passing through the aperture $F$ in unit time without, and later with, the collodion film gave the ratio of the effective areas with and without the film. It is possible that for the lower energy of the fluorine alpha-particles (as compared with that of the polonium particles) the opacity was slightly different. However, its value obtained as just described always agreed closely with that estimated from the area of visual blackness seen under the microscope. This fact, together with the way in which the films were made, substantiates the belief that the opacity was due to the presence of "large" dust fragments and not to variations of film thickness. The correction was typically from two to four percent. The yields measured with different films were concordant. The same window frame and film were used at all angles in obtaining the angular distribution of the alpha-particles.

**Solid-angle determination**

The effective diameter of the small hole $F$ was measured with a micrometer microscope to be 0.564 mm. Its mean distance to the center of the target-spot was determined with a micrometer depth gage to be 4.452 cm for the 90° port. These two measurements, together with a correction of one percent for the finite thickness of the small aperture and the finite size of the spot, resulted in a solid angle of $1.00\pm0.01\times10^{-5}$ of a sphere. It was slightly different at the other angles at which observations were made but in all cases was measured with similar accuracy.

This was the only geometric factor on which the results depended.

**Targets**

Thick natural crystals of calcium fluoride were used. Electrostatic charging of the crystal face[7] was reduced by a fine tungsten whisker which touched the face of the crystal just outside the bombarded area. Some charging was evident even then with a clean target surface but, in agreement with the experience of the Madison group, a few minutes' bombardment gave a sufficient layer of carbon to reduce the resistance drop along the surface to a negligible value.

Cleavage surfaces of the crystals were used. They were lightly scraped with a sharp knife at frequent time intervals to remove accumulated carbon. The surfaces were never ground or polished or brought into contact with any foreign matter which would be likely to become imbedded in them.

The possible effects of charging of the crystal and carbonization in reducing the effective bombarding voltage of the beam were guarded against by working at voltages sufficiently far

[7] E. J. Bernet, R. G. Herb and D. B. Parkinson, Phys. Rev. **54**, 398–408 (1938).

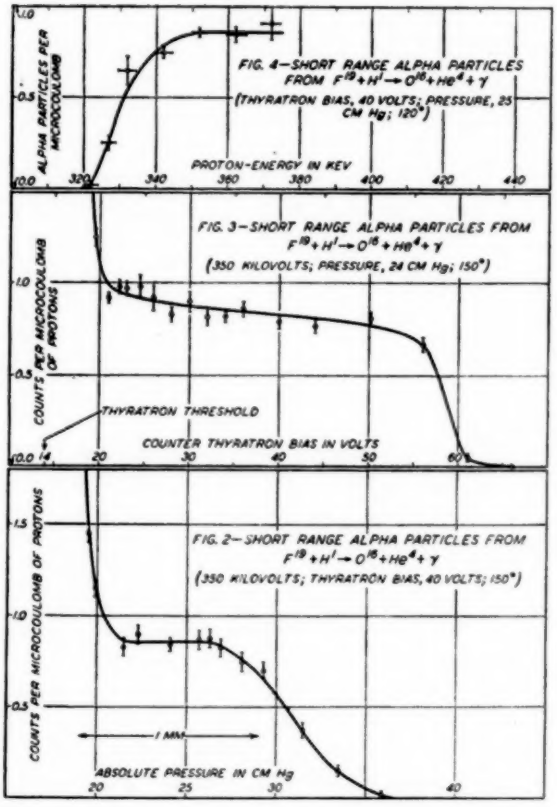
FIG. 4—SHORT RANGE ALPHA PARTICLES FROM $F^{19}+H^1 \rightarrow O^{16}+He^4+\gamma$
(THYRATRON BIAS, 40 VOLTS; PRESSURE, 25 CM Hg; 120°)
ALPHA PARTICLES PER MICROCOULOMB
PROTON-ENERGY IN KEV
FIG. 3—SHORT RANGE ALPHA PARTICLES FROM $F^{19}+H^1 \rightarrow O^{16}+He^4+\gamma$
(350 KILOVOLTS; PRESSURE, 24 CM Hg; 150°)
COUNTS PER MICROCOULOMB OF PROTONS
THYRATRON THRESHOLD
COUNTER THYRATRON BIAS IN VOLTS
FIG. 2—SHORT RANGE ALPHA PARTICLES FROM $F^{19}+H^1 \rightarrow O^{16}+He^4+\gamma$
(350 KILOVOLTS; THYRATRON BIAS, 40 VOLTS; 150°)
COUNTS PER MICROCOULOMB OF PROTONS
1 MM
ABSOLUTE PRESSURE IN CM Hg

FIGS. 2, 3, and 4. The number of counts per microcoulomb of protons as a function of pressure in the absorption cell (Fig. 2), bias on the grid of the input tube of the scaling circuit (Fig. 3), bombarding voltage (Fig. 4). Exploratory curves of Figs. 2 and 3 served to determine optimum operating values of pressure and bias. In Fig. 2 the horizontal arrow marked "1 mm" indicates the change in pressure necessary to change the stopping power of the absorption region $A$ by 1 mm of normal air at 15°C and 760 mm Hg. It can be seen that the region of complete separation of the alpha-particles and the scattered protons is about one-half of a mm air equivalent. The long range alpha-particles number about one-half percent of the short range alpha-particles and consequently do not appear here in measurable numbers.

above the 330-kv resonance to be safely on the horizontal portion of the yield-curve.

Two good quality $CaF_2$ crystals of different origin gave alpha-particle yields in agreement to within the accuracy of the measurements. A portion of one of them was examined for us by Dr. H. E. Merwin of the Geophysical Laboratory of the Carnegie Institution of Washington. He found that (1) the crystal was free from inclusions of foreign solid matter and of water and (2) its index of refraction differed less than 0.002 and its specific gravity less than 0.001 from other good specimens of mineral fluorite which he had selected over a period of several years. It can therefore be said that the crystals used in these measurements were representative of the best mineral crystals available. A quantitative chemical analysis for fluorine in fluorite is attended by such difficulties as to make any but a most painstaking analysis of very little value.

Targets prepared by the fusion or evaporation in air of compounds of fluorine were found to be unreliable for yield-measurements because heating the compounds in air reduced their fluorine content.

### Angular distribution and yield measurements

The number of counts recorded by the amplifier-scaler-counter circuit per microcoulomb of bombarding protons was a function of three arbitrarily variable conditions:

(1) The pressure in the absorption cell.
(2) The bias on the grid of the input tube of the scaling circuit.
(3) The bombarding voltage.

The way in which the alpha-particle yield was experimentally found depended on obtaining plateaus in the curves of the counts per microcoulomb against the above three variables. These plateaus are shown in Figs. 2, 3, and 4. The curves are typical of a considerable number taken at 60°, 90°, 120° and 150° with respect to the forward direction of the proton beam.

From the heights of the horizontal positions of these three curves, taken together, was determined the number of alpha-particles per microcoulomb of incident protons. Such a value was obtained for each of the above-mentioned angles.

For each angle the crystal face was set so its normal approximately bisected the angle between the beam and the observation port. This minimized the effect of roughness of the target surface.

It was not easy to make measurements at smaller angles than 60° due to the obliquity of the crystal and the preponderance of scattered protons.

## Results

After having corrected the results at the several angles for the slight differences of geometry and the transmission-factor of the

collodion film and for the motion of the center of mass, the values given in Table I were obtained. There is seen to be no systematic deviation from spherical symmetry. Thus the total yield over $4\pi$ steradians is

$8.9\pm0.5\times10^4$ short range alpha-particles

per microcoulomb of 360-kv protons bombarding a thick crystal of $CaF_2$.

The probable error has been set equal to the square root of the sum of the squares of the errors introduced by the components described below. Our largest error we estimate to be that introduced in reading off the number of alpha-particles per microcoulomb from the data. In the number-thyratron bias curves the plateau obtained was never exactly horizontal and one has to use his best judgment in deciding what value to select. We took the uncertainty in this process to be three percent. The uncertainties in the current averaging, the collodion film transmission factor, the area of aperture $F$, and its mean-square distance from the target all combine to give a total probable error of five percent. The long range alpha-particles from reaction ($c$) were found to represent less than one-half percent of the total alpha-particle yield at 360 kv. No correction was made for them.

In view of the evidence cited above, the yield of 6.2-Mev quanta is taken to be equal to the alpha-particle yield.

### Angular distribution of gamma-rays

In any experiment which does not use this radiation over the entire sphere it is important to know the angular distribution of the gamma-radiation. There are apparently sound theoretical reasons for expecting the radiation to be spherically symmetric. However, it was regarded as desirable to determine the actual distribution by measurement. The apparatus used for this purpose is shown in Fig. 5. The Geiger counter was placed in the heavy-walled lead box $E$. The box was mounted on a rigid framework whose axis of rotation passed through the target-spot and perpendicular to the beam. The front wall of $E$ was sufficiently thick (6.4 cm) to reduce the intensity of 6.2-Mev radiation to about four percent of its incident value, except over the area of the aperture, which had the shape of a circular cone with vertex at the target. The geometry was such as to make $\Delta\theta=7°$. It was verified that this was the actual aperture by observing the effect of inserting a long brass plug in the conical hole.

A Lauritsen electroscope was clamped in a fixed position with respect to the target and was used as a monitor for all measurements.

The angular distribution of the gamma-radiation from a thick target was determined for bombarding voltages of 370, 900 and 1000 kv. Reasons for selection of these voltages are evident from examination of the yield-curve.[7, 8]

At all three voltages the radiation was found to be spherically symmetric to within the experimental error of five percent.

TABLE I. *Alpha-particles per microcoulomb of bombarding protons observed at the various angles corrected for the motion of the center of mass and adjusted to the mean solid angle at 90°.*

| ANGLE IN THE LABORATORY SYSTEM | COUNTS PER MICROCOULOMB IN $1.00\times10^{-5}$ OF A SPHERE |
|---|---|
| 60° | $0.86\pm0.10$ |
| 90 | $0.87\pm0.02$ |
| 120 | $0.90\pm0.02$ |
| 150 | $0.89\pm0.02$ |

### Quantum intensity of gamma-radiation at 1050 Mev

As discussed above the gamma-ray energy is the same (with the exception of the slight amount of annihilation radiation described below) at all the resonances with which this work was concerned. Valid comparisons of the intensity of the radiation produced at various values of bombarding voltages can therefore easily be made with a Geiger counter or electroscope without attention to geometric conditions or to the nature or arrangement of the shielding. The ratio of the gamma-ray intensities at 370 kv and 1050 kv was carefully determined by simultaneous measurements with a Lauritsen electroscope and with a Geiger counter (Fig. 5). The two ratios always differed inappreciably.

Furthermore, the intensity ratio was found to be the same for moderate shielding (0.5 cm of lead over the sensitive area of the counter

[8] L. R. Hafstad, N. P. Heydenburg and M. A. Tuve, Phys. Rev. **50**, 504–514 (1936).

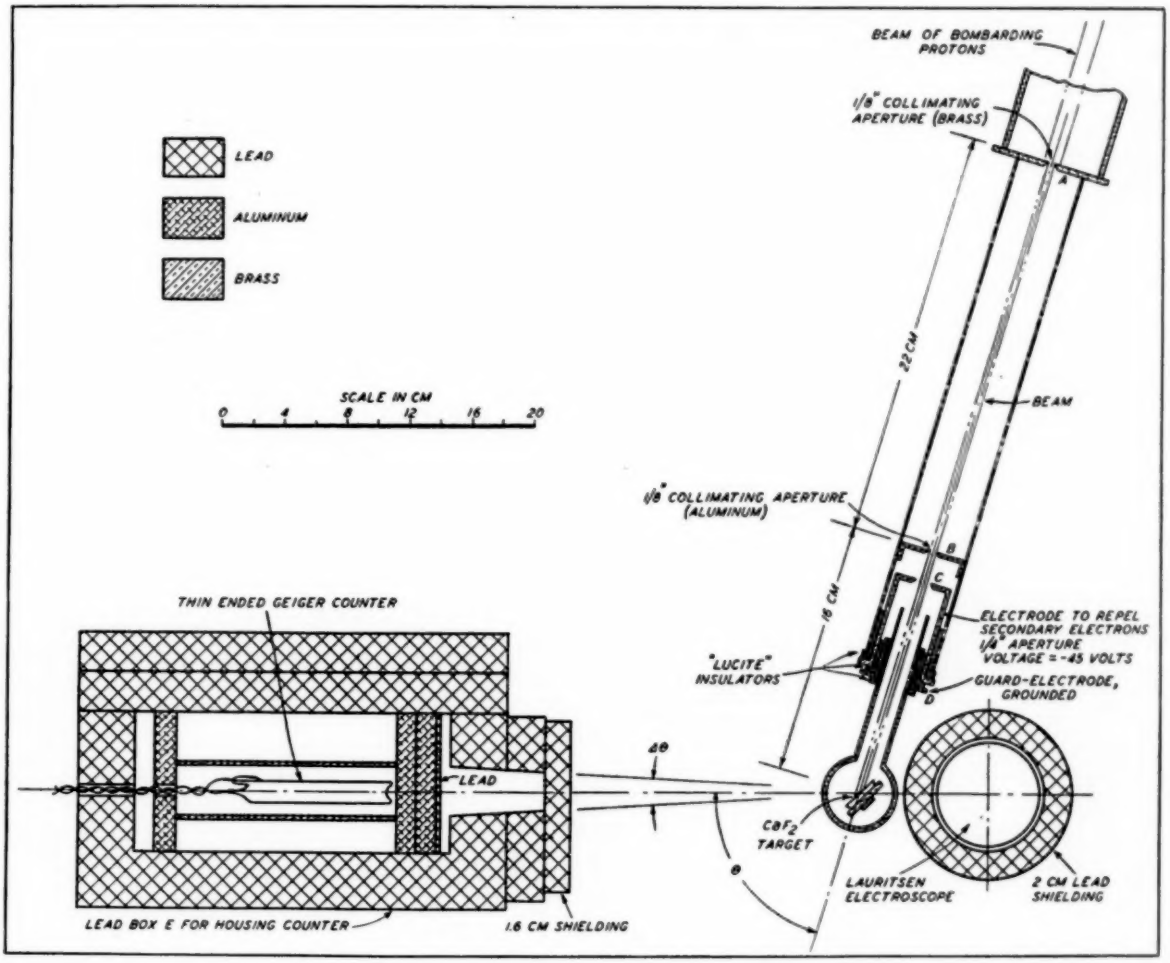


FIG. 5. Diagram of apparatus used to determine the angular distribution of gamma-radiation and the intensity at 1050 kv relative to that at 370 kv. For the angular distribution the lead marked "shielding" was not present. The ratio of the intensities was taken with and without the shielding with similar results.

and 0.3 cm of brass over the electroscope) and heavy shielding (2.0 cm lead for both the counter and electroscope). This assured that the results were not influenced by the presence of the slight amount of soft radiation from the annihilation of the positive members of the nuclear pairs which arise at the higher bombarding voltages.[9]

The average of all such determinations was

$$I_{1050\text{ kv}}/I_{370\text{ kv}}=42.0\pm0.8.$$

This is in good agreement with the earlier measurement (heavy shielding—one inch of lead) of 41.2 made in this Laboratory.[8]

Thus the yield of 6.2-Mev quanta from $CaF_2$ at 1050 kv is

$$3.7_4\pm0.2\times10^6 \text{ quanta}/\mu c \text{ of protons.}$$

## DISCUSSION

A rough check on the absolute quantum intensity at 360 kv was made by comparison with a milligram of radium shielded with three cm of lead. The efficiency of the aluminum-sheathed Geiger counter for each line of the radium spectrum and for the fluorine radiation was taken to be proportional to the product of the true absorption coefficient of aluminum by

[9] The Pasadena group estimates (private communication) the relative yield of pairs and gamma-ray quanta at 1 Mev to be approximately two percent. Since the sensitivity of detection of 6-Mev quanta is about four times as great as 0.5-Mev quanta, the maximum contribution of the annihilation radiation to the intensity ratio would be of the order of one percent for lightly shielded detectors and one-tenth percent for our heavily shielded ones.

the mean range of the secondaries.[10] Under these assumptions the number of quanta from the $CaF_2$ target per microcoulomb of protons is given by

$$Q_F = Q_{Ra}\left(\frac{C_F}{C_{Ra}}\right)\left(\frac{\sum_i p_i \tau_i R_i e^{-\mu_i z}}{\tau_F R_F e^{-\mu_F z'}}\right),$$

where $C_F$ and $C_{Ra}$ are the observed numbers of counts due, respectively, to one microcoulomb of protons bombarding fluorite and to one milligram-second of radium placed in the target position, $p_i$ is the relative intensity of the $i$th gamma-ray line of the radium spectrum, the quantities $\tau_i R_i$ are proportional to the counter efficiencies mentioned above, the exponentials take account of absorption in the lead shielding, $Q_{Ra}$ is the total number of quanta per second from a milligram of radium, and the summation is taken over the entire radium spectrum.

Using the best available values for all quantities involved in the above formula, and our ratio $(C_F/C_{Ra})$, we obtained a value for $Q_F$ differing by less than 20 percent from the alpha-particle count. In view of the crudeness of this type of calibration the agreement is regarded as satisfactory.

It is to be noted that a similar calculation made by us on data previously published by Hafstad and Tuve[11] of this Laboratory gives $2\times10^5$ quanta/$\mu c$ at 350 kv contrary—that is, about a factor of two too high instead of a factor of 1000 too small—to the commonly accepted interpretation of their data.[12]

The original estimate of McMillan[13] is in order of magnitude agreement with the intensity here reported.

Streib, Fowler, and Lauritsen[14] have recently made a Gray-Laurence type calibration of the fluorine source with an electroscope, whose sensitivity was determined by exposure to lightly shielded radium. Their thick-target result is $4.0\times10^6$ quanta/$\mu c$.

These measurements provide valuable independent checks of the quantum intensity, but in view of the complexity of the quantitative interpretation of ionization-chamber results, it appears that greater reliance can be placed on the direct alpha-particle count.

## Acknowledgments

We gratefully acknowledge the support of our Director, Dr. John A. Fleming, and the encouragement of Drs. M. A. Tuve, and L. R. Hafstad of this Laboratory. We are indebted to Dr. H. E. Merwin of the Geophysical Laboratory for the examination of one of the fluorite crystals used in this work. Professors C. C. Lauritsen and W. A. Fowler and Drs. J. F. Streib and R. A. Becker have discussed some of their experiments with us and have very kindly furnished in advance of publication recent data obtained in their laboratory.

[10] See, for example, W. Bothe and W. Genther, Zeits. f. Physik **106**, 236–248 (1937).
[11] L. R. Hafstad and M. A. Tuve, Phys. Rev. **48**, 306–315 (1935).
[12] H. A. Bethe, Rev. Mod. Phys. **9**, 207 (1937).
[13] E. McMillan, Phys. Rev. **46**, 868–873 (1934).
[14] J. F. Streib, W. A. Fowler and C. C. Lauritsen, Phys. Rev. **59**, 253–270 (1941).

# On the Thermal Activation of the Oxygen Molecule*

HOMER D. HAGSTRUM** AND JOHN T. TATE
*University of Minnesota, Minneapolis, Minnesota*

(Received December 16, 1940)

A study of the relative partial pressures of $O_2$ and the impurities $CO_2$, CO and $H_2O$ upon the temperature of a platinum filament operated in oxygen at low pressure (about $10^{-4}$ mm of mercury) has been made. The platinum filament was contained in the vacuum system of a mass spectrometer which was used as a partial pressure gauge. It was found that the partial pressure of oxygen began to fall at a filament temperature of approximately 1280°K and had dropped to 46 percent of its original value at 1740°K. This fall in the $O_2$ abundance was accompanied by rises in those of $CO_2$, CO and $H_2O$. Finally the effect completely disappeared. A number of considerations make it plausible that the process responsible for this effect involves the adsorption on the hot platinum filament of the oxygen molecules which on evaporation in activated form react with substances of *low* vapor pressure adhering to the glass envelope. The nature of the activation is most probably excitation to the metastable molecular states $^1\Delta$ and $^1\Sigma$. The dissociation of hydrogen by a hot tungsten filament has also been investigated and results in accord with previous work obtained.

IN the course of the study of electron impact processes in oxygen with a mass spectrometer[1] it was found that the abundances of the impurities $CO_2$, CO and $H_2O$ relative to $O_2$ depended on the temperature of the tungsten filament used as the source of electrons. These abundances could be changed by as much as a factor of 4 by varying the temperature of the filament in the range in which sufficient electron emission was obtained. It appeared that the generation of the gases was occurring in the spectrometer and that it depended on some sort of catalytic action of the hot filament surface. In this paper are discussed the procedure and results of an experiment designed to study this effect in oxygen in more detail. In addition the results of a study of the dissociation of hydrogen at a tungsten filament by the same method are presented.

## EXPERIMENTAL PROCEDURE

Any quantitative study of the effect in oxygen with the spectrometer alone was needlessly complicated since the filament was used both as the source of electrons and as the variable temperature catalyst. In addition the oxidation of the tungsten to form $WO_3$ occurred[2] very rapidly at the temperatures of satisfactory electron emission. To obviate these difficulties it was decided to study the formation of the gaseous oxides if it occurred using a platinum catalyst in the form of an auxiliary filament and to employ a relatively "cool" oxide-coated filament as the source of electrons in the spectrometer. The experimental arrangement is shown schematically in Fig. 1. Oxygen gas was allowed to leak into the system at a rate such that, with the diffusion pumps operating, the pressure in the collision chamber was about $10^{-4}$ mm of mercury. The mass spectrometer was used to determine the dependence of the relative partial pressures of oxygen and the impurities on the temperature of the auxiliary filament. This was done by observing the heights of the ion peaks of $O_2^+$, $CO_2^+$, $CO^+$ and $H_2O^+$. With this arrangement it was possible not only to determine the abundance of an ion relative to that of another at a particular temperature of the auxiliary filament but also relative to the abundance of the same ion at any other temperature.

The temperature of the auxiliary filament was measured with an optical pyrometer and the temperature-resistance characteristic of the filament determined. The voltage drop across the filament and the current through it as well as their ratio were checked at each setting. In this manner any change in the filament such as might be caused by evaporation or chemical attack by the surrounding gas and which results in a change of resistance could be detected. Heat loss by

* A report of this work was presented at the Washington Meeting of the American Physical Society, April 26, 1940. H. D. Hagstrum and J. T. Tate, Phys. Rev. **57**, 1071A (1940).

** Now at the Bell Telephone Laboratories, New York.

[1] H. D. Hagstrum and J. T. Tate, Phys. Rev. **59**, 354 (1941).

[2] I. Langmuir, J. Am. Chem. Soc. **37**, 1139 (1915).

conduction at the low gas pressures used in this experiment was negligible.

The entire vacuum system was baked out thoroughly and the filaments outgassed under vacuum. When no gas was being admitted and both the auxiliary and spectrometer filaments were on, the residual partial pressure of any impurity was less than about $10^{-7}$ mm of mercury.

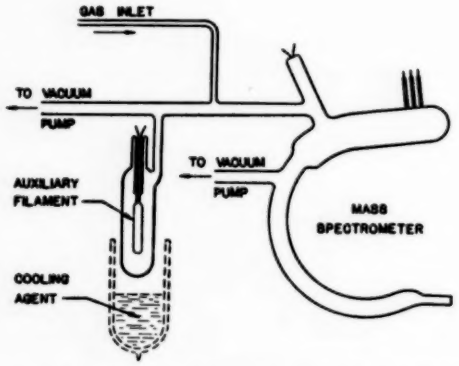


FIG. 1. Schematic diagram of the experimental arrangement. For details of the mass spectrometer see the reference of footnote 1. The volume of the collision chamber, bulb containing the auxiliary filament and connecting leads is approximately 4 liters. This is evacuated by a two-stage mercury diffusion pump of the Langmuir type. The pump on the analyzer chamber also draws gas from the collision chamber through the second ion slit ($0.022 \times 0.8$ cm). The auxiliary filaments are 16 cm long and have the diameters: platinum 0.275 mm, tungsten 0.193 mm. Provision was made to immerse the bulb containing the auxiliary filaments completely in a cooling agent.

## RESULTS

A graph of the experimental results is shown in Fig. 2. The height of the $O_2^+$ peak remained constant as the temperature of the platinum filament was increased up to about 1280°K. At this temperature the partial pressure of $O_2$ began to fall. At 1740°K it had dropped to about 46 percent of its original value. The magnitude of the effect is thought to be rather remarkable. This drop in the abundance of $O_2$ was accompanied by rises in the abundances of $CO_2$, CO and $H_2O$. (See curve 2 of Fig. 2.) In Table I are given the heights of the ion peaks of $O_2^+$, $CO_2^+$, $CO^+$ and $H_2O^+$ with and without gas being admitted and with and without the auxiliary filament on. The heights are given relative to the height of the $O_2^+$ peak with oxygen being admitted and the filament at room temperature.

The effect persisted in the same manner when the bulb containing the auxiliary filament was immersed in liquid air except that the increases in the abundances of $H_2O$ and $CO_2$ were obliterated. It was found that the results were reproducible within the limits of error involved in the peak height measurements and the adjustment of the filament temperature. Finally, however, the effect vanished, the abundances of $O_2$, $CO_2$, CO and $H_2O$ becoming completely independent of the temperature of the auxiliary filament. It is estimated that had the filament been operated continuously at the temperature at which the partial pressure of $O_2$ was reduced to one-half, the effect would have lasted a length of time of the order of a very few minutes.

## DISCUSSION

When the auxiliary filament was hot enough the bulb acted as a sink for oxygen molecules. Not all of the oxygen which disappeared in molecular form reappeared in the $CO_2$, CO and $H_2O$, however. It is suggested that the mechanism of the process involves activated adsorption[3] of the oxygen molecules on the hot platinum surface. These molecules on evaporation in activated form react with substances of *low* vapor pressure containing H and C adhering to

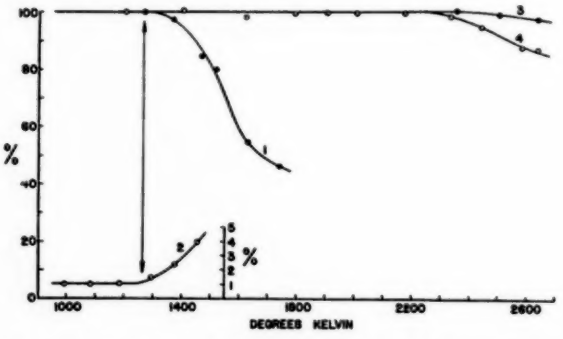


FIG. 2. Variation of ion peak height with temperature of the auxiliary filament. Curves 1 and 2 show the variation of the heights of the $O_2^+$ and $CO_2^+$ peaks, respectively, with the temperature of the auxiliary platinum filament with oxygen in the system at a pressure of about $10^{-4}$ mm of mercury. Curve 3 shows the variation of the height of the $H_2^+$ peak with the temperature of the auxiliary tungsten filament. The pressure of hydrogen in the system was approximately $10^{-4}$ mm and the glass bulb was at room temperature. Curve 4 is for the $H_2^+$ peak with the bulb immersed in liquid air. The traps of the diffusion pumps were immersed in liquid air during all of these experiments.

[3] A discussion of activated adsorption has been given by H. S. Taylor, J. Am. Chem. Soc. **53**, 578 (1931).

TABLE I. *Relative abundances of* $O_2$, $CO_2$, CO *and* $H_2O$.

| | $O_2$ | $CO_2$ | CO | $H_2O$ |
|---|---|---|---|---|
| No gas admitted—Pt filament off | — | 0.018 | 0.034 | 0.027 |
| No gas admitted—Pt filament at 1615°K | — | 0.018 | 0.035 | 0.030 |
| Oxygen admitted—Pt filament off | 100 | 0.475 | 0.161 | 0.072 |
| Oxygen admitted—Pt filament at 1615°K | 55 | 8.42 | 0.392 | 0.169 |

the glass walls of the bulb to form in part at least the gaseous oxides $CO_2$, CO and $H_2O$. In support of this suggestion the following considerations are presented:

1. It is not likely that the effect can be attributed to the reaction of oxygen with substances occluded in the filament as it had been very thoroughly outgassed and emitted a negligible amount of impurity when heated to a high temperature with no oxygen present. (See Table I.)

2. The effect cannot be attributed to the reaction at the hot filament surface of $O_2$ with other gases containing H and C. No such gases present in sufficient quantity could be detected with the mass spectrometer. Furthermore, one should expect such a process to continue as long as the same gas is admitted to the spectrometer and the filament run at a high enough temperature.

3. The only remaining site for the production of the impurities is the glass wall. The dependence of the occurrence of the process on the presence of a hot filament suggests activation of the oxygen. The disappearance of the effect may be attributed to "clean-up" of the glass walls. It is to be emphasized that the substances adhering to the walls must have been of very low vapor pressure since the effect persisted after baking the glass under vacuum sufficiently to make the system clean enough for ordinary mass spectrometric work.

There are three possible types of activation which the oxygen can undergo on being adsorbed and subsequently evaporated at the hot platinum surface. These are:

1. Excitation to either or both of the metastable molecular states $^1\Delta_g$ and $^1\Sigma_g^+$. These states lie approximately 1.0 and 1.6 volts above the ground electronic state of the molecule.

2. Excitation into higher vibrational levels which are to be considered as metastable.[4] These states would lie near the dissociation limit of the molecule at 5.082 volts.

3. Dissociation of the molecule into atomic oxygen. The heat of dissociation of $O_2$ is 5.082 volts.

Since the first of these processes involves the least *true* activation energy it most likely will also exhibit the least *apparent* activation energy[5,3] and will thus predominate at lower temperatures.

Langmuir's study[6] of the mechanism of the catalytic action of platinum on the reactions $2CO+O_2=2CO_2$ and $2H_2+O_2=2H_2O$ indicates that oxygen is adsorbed "in the form of single atoms combined with separate platinum atoms" and that "this chemical union is so firm that there is no appreciable evaporation of the oxygen atoms from the surface even with the platinum at 1500°K." Since the auxiliary filament in the present experiment was operated in an atmosphere of practically pure oxygen at temperatures not greatly exceeding 1500°K it must have possessed a film of adsorbed oxygen atoms covering almost the entire surface. If the liberation of atomic oxygen by the filament were responsible to any appreciable degree for the formation of the impurities $CO_2$, CO and $H_2O$ one should expect that a part of the atomic oxygen would condense on the glass walls like hydrogen atoms. Langmuir[2] has obtained evidence that an active form of oxygen which he considers to be atomic oxygen can be collected on glass. He states that the phenomenon resembles in many ways that observed in hydrogen. It is to be expected that, as in the case of hydrogen, this condensation is enhanced by cooling the glass to the temperature of liquid air. The failure to observe any significant change in the effect when the bulb containing the auxiliary filament was immersed in liquid air and the fact that the effect finally vanished *completely* are taken as evidence that

[4] See G. Herzberg, *Molecular Spectra and Molecular Structure, I. Diatomic Molecules* (Prentice-Hall, New York, 1939), p. 514.

[5] See C. N. Hinshelwood, *The Kinetics of Chemical Change in Gaseous Systems* (Oxford, 1933), Chapter IX, p. 348 ff.

[6] I. Langmuir, Trans. Faraday Soc. **17**, 607, 621 (1921–22).

atomic oxygen is not involved. The most probable activation of the molecule is excitation to the metastable states $^1\Delta$ and $^1\Sigma$.

In view of Langmuir's observation[6] of a very tenaciously held layer of atomic oxygen on platinum the following possibilities are suggested for the mechanism of the adsorption process observed in the present work:

1. Two oxygen atoms simultaneously evaporated from adjacent elementary spaces on the platinum surface combine to form an excited oxygen molecule. This possibility is to be regarded as improbable in view of Langmuir's observation that no appreciable evaporation of oxygen atoms occurs even with the platinum at 1500°K and because it necessitates the simultaneous evaporation of atoms occupying adjacent elementary spaces on the metal surface.

2. The oxygen molecule is adsorbed in a second layer on top of the layer of atomic oxygen and is subsequently evaporated in a metastable excited state. The molecule which is evaporated from the surface may be the same molecule which was adsorbed. On the other hand, the molecular structure of the oxygen which is adsorbed in the second layer may be broken up, each atom combining with an atom of the first layer to form an excited molecule which later evaporates. A molecule held to the metal surface in this manner would, by virtue of its small stray field of force[7] be very much more weakly bound than an unsaturated oxygen atom and would evaporate more readily.

3. The oxygen molecule is adsorbed in a single vacant elementary space in the layer of adsorbed atomic oxygen and later evaporates in an excited state. This mechanism would necessitate evaporation of atomic oxygen from the filament above 1280°K in sufficient quantity to provide sites for adsorption of the molecular $O_2$. An oxygen molecule striking two adjacent elementary spaces which are vacant would in all probability dissociate into atoms and become a part of the adsorbed atomic layer.

Because it does not require any appreciable evaporation of atomic oxygen from the platinum surface the second of these three proposed mechanisms is considered to be the most probable. Langmuir's work[6] has shown that the adsorbed film of atomic oxygen is very active chemically reacting with a molecule of CO which strikes it to form $CO_2$. Thus it appears likely that it should react with oxygen atoms adsorbed in a second layer to form molecules which, if the temperature is high enough, may be excited.

The generation of the oxides $CO_2$, CO and $H_2O$ which has been studied using a platinum catalyst was first observed as the result of the presence in the spectrometer of a hot tungsten filament Thus the adsorption of oxygen molecules involving activation must also occur on tungsten. Langmuir[6] has found that atomic oxygen is adsorbed on tungsten in much the same way as on platinum. In addition to the process which results in the formation of the gaseous oxides in the case of tungsten the metal itself is oxidized to form $WO_3$ as is well known.[2]

## Dissociation of Hydrogen

The dissociation of hydrogen by a heated tungsten filament was also investigated by the method described in this paper. This study was undertaken primarily as a check on the method as there are data from other sources with which the results may be compared. Curve 4 of Fig. 2 shows the dependence of peak height of the $H_2^+$ ion on the temperature of an auxiliary tungsten filament with the bulb containing the filament immersed in liquid air. (See Fig. 1.) The temperature of 2280°K at which dissociation of the hydrogen first proceeds at a measurable rate agrees reasonably well with the temperature observed by Langmuir and Mackay[8] at which the rate of heat loss from a tungsten wire in hydrogen departs from that calculated on the simple theory of conduction of heat through gases.

It was essential that the bulb containing the auxiliary filament be immersed in liquid air for an effect as large as that indicated by curve 4 of Fig. 2 to be observed. After operating the filament at the high temperature for a length of time of the order of a minute the height of the

[7] I. Langmuir (reference 6) has suggested that the low boiling point and the relatively small adsorption of oxygen by surfaces of glass and mica (I. Langmuir, J. Am. Chem. Soc. **40**, 1361 (1918)) indicates a small stray field of force for $O_2$.

[8] I. Langmuir and G. M. J. Mackay, J. Am. Chem. Soc. **36**, 1708 (1914).

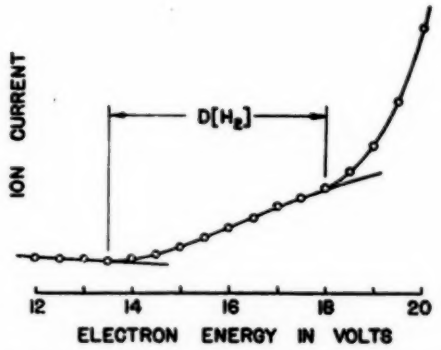


FIG. 3. Dependence of the $H^+$ ion current from $H_2$ on impacting electron energy in the range 12 to 20 volts for high gas pressure and hot spectrometer filament.

$H_2^+$ peak rose to approximately that given by curve 3 of Fig. 2 at the same temperature. The original magnitude of the effect could be restored, however, by removing the liquid air, warming up the bulb and replacing the liquid air. This observation agrees with that of Langmuir[9] who attributed the effect to saturation of the glass walls with atomic hydrogen which had been evaporated from the filament and which was released when the wall was warmed.

Langmuir[9] also observed that some of the hydrogen could remain in atomic form sufficiently long to reach a trap cooled by liquid air at some distance from the filament. This phenomenon undoubtedly explains curve 3 of Fig. 2.

Evidence that hydrogen can persist in atomic form was obtained in another manner by measuring the appearance potential of $H^+$ ions with a very hot tungsten filament in the mass spectrometer and the pressure of hydrogen raised to about $10^{-3}$ mm of mercury. The spectrometer does not have differential pumping on the filament so that the gas around the filament can reach the collision chamber. The only direct path from the filament by which an atom can reach the collision chamber without suffering a collision with the glass envelope or the metal parts of the spectrometer, however, is through the defining slit of the electron beam ($0.01 \times 0.5$ cm). The variation of the $H^+$ ion current with energy of the impacting electrons in the range of 12 to 20 volts is shown in Fig. 3. $H^+$ ions from the dissociation of the molecule by electron impact appear at 18 volts.[1] However, under the conditions existing when these data were obtained $H^+$ ions also appeared at 13.5 volts or approximately the ionization potential of the hydrogen atom. This indicates that the gas in the collision chamber of the spectrometer consisted partly of atomic hydrogen. The ionization below 18 volts disappeared when a cooler filament was used with the same gas pressure. This fact together with the results of a study of the relative abundances of the impurities present in the system indicates that the effect is not due to $H^+$ ions from the dissociation of an impurity.

Determination of the quantities of gas involved in the processes studied was not attempted. A rough idea of the magnitude of the effects may be gotten from the pressure used and the facts concerning the vacuum system and auxiliary filaments given in the caption of Fig. 2.

The mass spectrometer has been used extensively as a very sensitive gas analyzer. It is suggested that it may also be used, as in the experiments described in this paper, to "observe" gaseous reactions at low pressures on metal surfaces *as they occur*. Technical improvements of the apparatus and procedure might include simplification of the geometry of the vacuum system, placing the auxiliary filament nearer the spectrometer, perhaps in the collision chamber, introduction into the vacuum system of special surfaces to react with products of evaporation from the auxiliary filament and cutting off of the spectrometer from the vacuum pumps and gas inlet system during the course of an experiment.

[9] I. Langmuir, J. Am. Chem. Soc. **34**, 1310 (1912).

# Influence of a Longitudinal Magnetic Field on an Electrical Discharge in Mercury Vapor at Low Pressure

CHARLES S. CUMMINGS* AND LEWI TONKS
*Research Laboratory, General Electric Company, Schenectady, New York*
(Received October 28, 1940)

The effect of a uniform longitudinal magnetic field on a low pressure arc has been investigated in an arc tube with a Hull type cathode and movable and fixed probes. The magnetic field collimated the current flow from the cathode into a luminous beam which disappeared rather abruptly 30 cm from the cathode into a tube-filling glow. This glow was more intense at the axis than in the absence of field. By making the field more intense at the cathode the beam was made to fill the tube and the subsequent glow was indistinguishable from that observed in the absence of field. It thus appeared that a uniform field exercised no constrictive effect on the arc. Distortion of the probe characteristics by the field limited the range within which the probes could be used to low field values at which interesting magnetic effects were still weak. It was demonstrable that the field imparted a transverse stiffness to the arc which caused the transmission of a disturbed condition over large distances in the direction of electron flow. The measurements showed that there was no marked change in electron temperature, gradient, or electron concentration in the presence of a field, and indicated that the limiting cross-sectional distribution of charge as transmitted disturbances die out is the same as in the absence of field. The change of transverse potential distribution with field was found to be roughly in accordance with the modified Boltzmann distribution for the electrons which was previously derived theoretically.

## I. INTRODUCTION

IN a recent paper Tonks[1] developed a theory of the effect of a longitudinal magnetic field on a low pressure arc. The experiments to be described constitute a test of the adequacy of the theory.

Rokhlin[2] has investigated some aspects of the same problem. Otherwise practically no significant work has been reported in the literature. Some of the effects sought are small and are frequently obscured by complicating circumstances. In particular, the theory of probes in the presence of a magnetic field is not in a satisfactory state, although the attempt has been made to develop one,[3] so that probe methods fail to give interpretable results in interesting ranges.

This paper consists of three main divisions. In the first the large scale and visible effects of the field will be discussed. The second will be devoted to the experimental results obtained from probe characteristics and will involve such questions as the effect of the magnetic field on the plasma potential distribution, arc gradient, electron temperature, and electron current density distribution. Part 3 will then be devoted to calculations on the basis of these data and a comparison of theory and experiment.

## II. APPARATUS

The experiments were carried out with a cylindrical glass discharge tube pictured in Fig. 1. The tube had an eight-celled, cylindrical, unipotential oxide-coated cathode 2.5 cm in diameter. The axis of the tube was horizontal and lay in the north-south direction, the cathode being to the north.

The mercury vapor pressure in the tube was controlled by the temperature of a small pool of mercury in the appendix at the cathode end of the tube. In all of the work here reported the condensed mercury temperature was 38.6°C, corresponding to a mercury vapor pressure of $5.4\times10^{-3}$ mm.

To prevent mercury vapor from condensing anywhere but in the thermostated appendix, small heaters were wound around the side arms that supported the probes and also around the bend at the upper end of the appendix. At the arc current employed (4 amperes) it was not necessary to place heaters about the main part of the tube since the energy dissipated by the arc sufficed to keep the temperature of the walls above 70°C.

* Now with Remington Arms Co., Bridgeport, Conn.
[1] Lewi Tonks, Phys. Rev. **56**, 360 (1939).
[2] G. N. Rokhlin, J. Phys. USSR **1**, 347 (1939).
[3] G. Spiwak and E. Reichrudel, Tech. Phys. USSR **5**, 715 (1938).

Of the four probes, which are shown in Fig. 1, Nos. 1 and 3 were fixed cylindrical probes of tungsten wire 0.00249 cm in diameter. Number 1 was 1 cm long, number 3 was 1.02 cm long. Probe number 4 was a flat wall probe of molybdenum 1.27 cm square. Number 2 was a tungsten wire probe 0.00250 cm in diameter and 9 mm long. By means of a small magnet this probe could be moved to any position along a horizontal diameter of the tube. Five standard positions were chosen for measurements, Nos. 1 and 5, 1.75 cm off the axis; Nos. 2 and 4, 0.87 cm off the axis; and No. 3 on the axis.

All of the probes were mounted perpendicular to the tube axis. Had the probes lain along the axis all of the current paths to them would have been perpendicular to the axial magnetic field which would, therefore, have offered maximum resistance to the electron flow. A transverse probe, however, offers one direction of approach which is parallel to the lines of force, so that its characteristics will be less affected by the field. The transverse probe was used as a compromise between this factor and the greater sampling accuracy of the axial probe.

That the transverse position of even the movable probe does not contribute markedly to the inaccuracy can be seen from the following considerations. When the probe lies at the center of the tube its center lies at a maximum of potential and electron concentration. Hence the average of these quantities in that neighborhood differs only slightly from the value at the axis. When the probe is near the tube wall the difference in radial distance of probe center and ends is small, so that the average is again not far off.

At first considerable difficulty was experienced with contamination of the probes by adsorbed oxygen which gave rise to irregularities in the characteristics. The same difficulty has been met with previously.[4] The remedy adopted was to sputter the probe for various lengths of time ($\frac{1}{2}$ min. to 5 min.) at 20 volts with respect to space potential before taking each reading. Even after this treatment deviations of the characteristic curves from the ideal shape have been observed to occur. These are thought to represent some complicating conditions in the arc not accounted for by the present arc or probe theory. The total sputtering during the course of the experiment was not sufficient to reduce the probe diameter appreciably.

[4] E. S. Lamar and K. T. Compton, Phys. Rev. **9**, 1069 (1931); A. L. Reimann, Phil. Mag. **20**, 594 (1935).

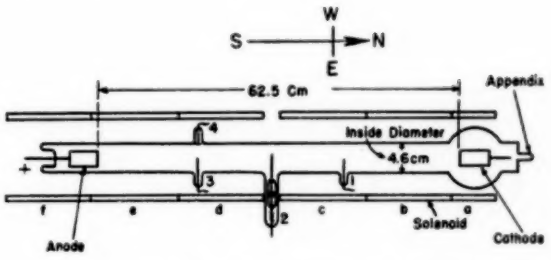


FIG. 1. Arc tube and magnetic field solenoid.

The usual technique of taking and interpreting probe characteristics was employed. From a plot of the logarithm of the probe current against the probe voltage curves were obtained from which the various arc characteristics were determined either directly or by calculation. Space potentials were obtained from the position of the break in the upper part of the curves. The diameters of the cylindrical probes were too large to allow them to be calculated from an $i^2$ *vs.* $V$ curve.

The magnetic field was obtained from a solenoid consisting of five short sections each 15.2 cm long by 12.6 cm in diameter having 147 turns apiece and one section, coil "*a*" in Fig. 1, 7.6 cm long with 74 turns. The arrangement of these coils with respect to the tube is shown in the same figure. When run in series they gave a field of 12.1 oersteds per ampere. It was possible to excite coil "*a*" independently of the rest. This enabled us to change the configuration of the field in the neighborhood of the cathode.

## III. Qualitative Aspects

When all the coils were connected in series and a current passed through them, a portion of the arc extending from the cathode toward the movable probe became concentrated into a definite beam. The arc here became much brighter than before, the brightness increasing toward the axis. A brightness pattern corresponding to the eight vanes of the cathode was observed to persist along the axis of the tube for

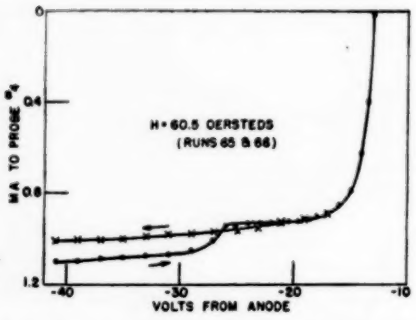


FIG. 2. Ion current anomaly due to transmission of cathode current redistribution.

the length of this beam, a distance of about 30 cm. Rather abruptly, within a space of 3 or 4 cm pattern and beam both disappeared into a tube-filling glow which persisted to the anode. The distribution of luminosity in this glow was less uniform than in the absence of magnetic field, the brightness being markedly more intense toward the axis.

Higher fields did not have any appreciable effect in extending the length of the beam although the sharpness of the pattern in it was improved by stronger fields. On the other hand, decreasing the pressure of the mercury vapor in the tube did increase the length of the beam.

At zero field a uniform glow filled the whole tube including the region behind the anode. At high fields ($\sim$120 oersteds) the glow behind the anode disappeared.

A magnetic field tends to constrain electrons to drift along the lines of force by decreasing their mobility in directions perpendicular to the field. Thus the longitudinal magnetic field caused the initial distribution of electrons at the cathode to persist toward the anode for a distance dependent primarily on the pressure in the tube.

An irregularity in probe behavior was traced to this longitudinal transmission of electron distribution. Occasionally a positive ion current-characteristic taken with the wall probe showed a step which was not reproducible. Figure 2 is an example. The points were taken in the order shown by the arrows. This effect could be explained by a redistribution of emission among the cathode sectors (which is not unusual) coupled with the partial transmission of such a redistribution down the arc.

As a check on whether sufficient transmission persisted beyond the well-defined beam, the following test was made. The wall probe was held so negative with respect to the plasma that only positive ions were reaching it. With no current in the solenoid, a permanent horseshoe magnet was held near the cathode. It caused a small increment (or decrement) in the probe current. The magnet was then held against the arc tube at an equal distance on the anode side of this probe. The effect of the magnet was approximately the same for both positions as well as for other positions which gave the same field at the probe. This showed that the field of the magnet was influencing the arc at the probe directly. On the other hand, in the presence of a longitudinal field of some 50 oersteds, the magnet near the cathode had a much greater effect than without the field, but away from the cathode it had about the same effect. This demonstrated the transmission of a disturbance at the cathode along the arc as far as the wall probe.

A real difficulty arises regarding the nature of the concentrated plasma in the beam. The thickness of the wall sheath precludes any but minute positive ion currents across it from plasma to wall. This points immediately to an essential difference between this arc plasma and a plasma that fills the arc tube. What happens to the ions formed, why they do not flow radially outward, whether there is an increasing portion of the arc current carried by the ions as the cathode is approached, and so on, are all questions which it is not possible to answer now.

It may be that the length of the beam portion of the arc is such that enough primary electrons penetrate to its end without inelastic collisions to maintain the necessary rate of ionization. There would then be little gradient in the beam, and only beyond its end would the gradient rise

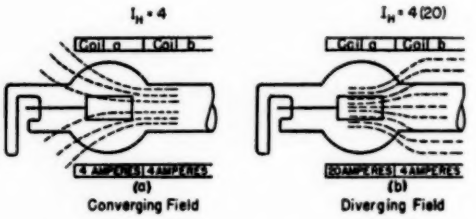


FIG. 3. Schematic diagrams of field configurations at cathode for two arrangements of coil currents.

to the value necessary for maintaining the electron temperature. Thus, in the beam, the energy for ionization would come from the cathode drop, while beyond the beam this energy would be supplied by the gradient.

Until recently the idea has been prevalent that an arc constricts in a uniform longitudinal field. This belief has been questioned by Tonks on theoretical grounds[1] and has been refuted by Rokhlin's experiments.[2] The present experiments give additional proof that a uniform longitudinal magnetic field does not constrict the arc, for, as has been mentioned, the arc actually spreads from the narrow beam into the tube-filling arc in such a field. The constrictions that have been observed in the past undoubtedly arose from a converging magnetic field and persisted by virtue of the transmission effect which has been discussed above. In the present experiments, except for a slight convergence of the field near the cathode, the arc lies in an essentially uniform field throughout its length (Fig. 3(a)).

If, on the other hand, the field at the cathode is given the proper divergence from a strong field to a uniform field of the same intensity as before, as sketched in Fig. 3(b), the arc is observed to expand from the cathode and fill the tube; also a normal distribution[5] of electron current is obtained. This matter will be discussed more quantitatively in the next section under the heading of random electron current distribution and the "peaking" effect.

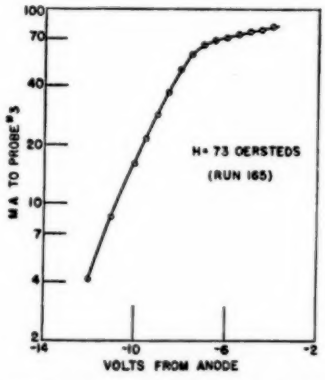


FIG. 4. Wall probe characteristic distorted by magnetic field.

[5] The term "normal distribution" as used here refers to the distribution found in the zero field case and is not necessarily synonymous with the Bessel distribution predicted by the general arc theory.

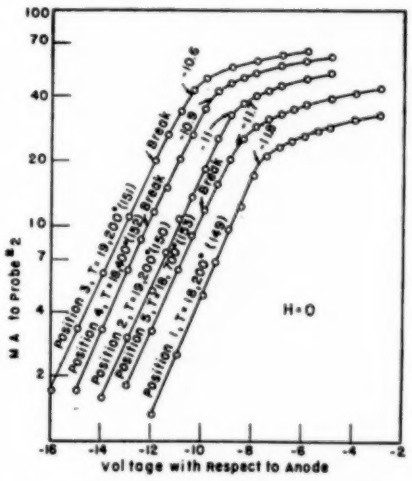


FIG. 5. Probe characteristics along arc diameter—no field. Successive curves are displaced 1 v to separate them. Space potentials in volts are attached to the break in each curve.

## IV. EXPERIMENTAL RESULTS

### a. General considerations

The arc was investigated under the following magnetic field conditions: (1) zero field, (2) 4 amp. in the coils (48.4 oersteds), (3) 6 amp. in the coils (72.6 oersteds), and (4) 20 amp. in coil "*a*" and 4 amp. in the rest of the coils. Figure 3(a) illustrates schematically the nature of the fields involved in (2) and (3) whereas Fig. 3(b) illustrates case (4). Many of the probe characteristics show deviations from the ideal form, and this requires some discussion.

At high magnetic fields (72.6 oersteds) the characteristics (log $i$ *vs.* $V$) do not have a straight portion. They do not even consist of two straight sections, but are considerably rounded throughout their length. This is well illustrated in Fig. 4. At this field strength the ordinary probe theory is no longer adequate. Space potential cannot be estimated from these curves to better than $\pm 0.5$ volt, and no reliable estimate of electron temperature can be made. In view of the inadequacy of probe theory no further calculations have been attempted at this field strength. Needless to say, it would be desirable to have a probe theory that would make interpretation of such results possible.

According to present theory the semilog probe characteristics taken at points across a diameter

of the arc should coincide in their straight portions. The zero magnetic field characteristics shown in Fig. 5 fulfill this requirement only partially. Their slopes are nearly the same so that they agree in electron temperature. If they were plotted on the same voltage scale, the straight portions of the curves for positions 3, 4 and 5 would coincide, but that for position 1 would lie 10 to 20 percent below the curve for position 2 and the latter 5 to 10 percent below the curve for position 3. The significance of this is not clear.

One of the most noticeable characteristics of the zero field curves is the apparent existence of a "break" in the curves. This shows that the electron velocity distribution deviates from the Maxwellian so that the concept of temperature becomes approximate. The value of $T_e$, which is required for calculations, has been taken from the lower portions of the curves where the difference in slopes is least.

The experimental points are not accurate enough to fix exactly the nature of the deviation from the ideal form, but they do show the existence of some anomaly. The deviations from the ideal form of the curves at 48.4 oersteds, as seen in Fig. 6, are still more marked but they are not so great that an estimate of the electron temperature cannot be made. Fortunately the irregularities in these curves do not seriously affect the determination of space potentials and random electron currents as they do in the 72.6-oersted case.

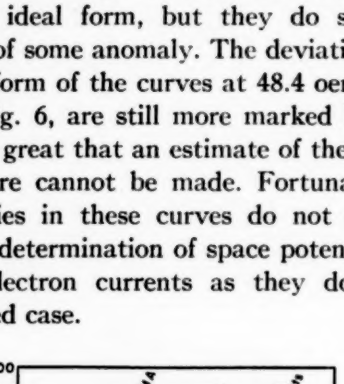


FIG. 6. Probe characteristics along arc diameter with field. Runs 159–163 with $I_H=4$, run 175 with $I_H=4(20)$.

**b. Random electron current and peaking effect**

Figure 7 is a plot of the random electron current to the probe as a function of the position of the probe along the tube diameter for the cases of zero field and 48.4 oersteds. It is seen that, in the presence of a magnetic field, there is a very considerable "peaking" with respect to the normal distribution curve. Furthermore, characteristics taken at the wall probe (No. 4) show a decrease in electron current to the wall when a magnetic field is applied. It is significant also that at probe No. 3 the increase in random current density was only about half as great as at probe No. 2. It seemed probable that the abnormal electron density was caused by transmission from the concentrated beam especially as it decreased with distance along the arc. It should then be possible by spreading the arc at the cathode with a suitable field configuration there to achieve a normal distribution of electrons in the arc which should persist down it.

To test this, a current of 4 amperes was maintained in all coils except coil "*a*." The current in this coil was raised to 20 amperes.

FIG. 7. Relative electron densities across arc without and with magnetic field.

This arrangement is designated by "4(20)." It gave rise to the type of field illustrated in Fig. 3(b). The immediately obvious effect was the filling of the tube near the cathode by the arc so that the cathode beam was absent. The glow was uniform and in general the external appearance of the arc throughout its whole length was quite indistinguishable from that in the zero field case. Probe measurements bore out the similarity. Runs on probe No. 4 showed

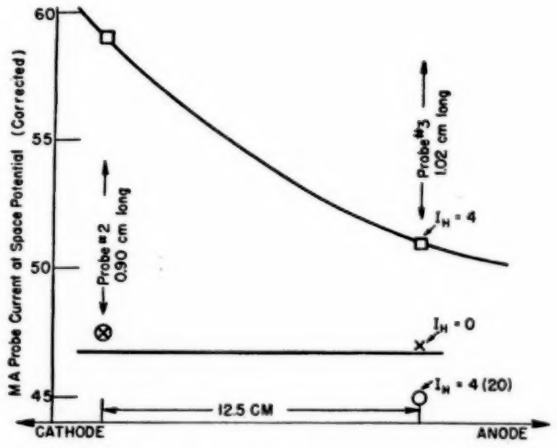


FIG. 8. Variation of axial electron concentration along arc with no field, with uniform field, and with field modified to give a normal distribution. The probe currents, corrected to the length of probe No. 3, are proportional to concentration.

no appreciable difference in wall current between zero field and the 4(20) field. Runs on probes No. 2 and No. 3 showed that at both places the random electron current density at the center of the arc had been reduced to its normal value. The effects of the fields zero, 4 and 4(20) are illustrated in Fig. 8.

Taken together, these facts are in accord with the theory that the normal distribution of electrons is characteristic of an arc in its steady state even in the presence of a magnetic field. Incidentally, the approach of an abnormal distribution toward a normal one is capable of theoretical treatment.[6]

It is unfortunate that time did not permit a more complete exploration of the 4(20) case, so that in what follows we must rely on the less satisfactory comparisons between the zero and 4-amp. field cases.

It will be seen in Fig. 7 that the random electron current distribution curve for the zero field case is unsymmetrical with respect to the tube axis. This is probably due to the vertical component of the earth's magnetic field which would tend to displace the arc toward the west, that is, to the right in the figure. On the other hand, the distribution for 48.4 oersteds is practically symmetrical. In this case the resultant magnetic field dips only about 0.7° with respect to the axis of the tube. Thus, in tending to follow the lines of force, the electrons would build up an asymmetry in a vertical rather than a horizontal plane. But the effect is probably too small to be detected even had we been equipped to neutralize the earth's field at our apparatus.

[6] This is developed in the next paper.

### c. Total number of electrons in cross section

From the data of Fig. 7 it was possible to make a rough estimate of the total number $N_e$ of electrons in unit length of cross section of the arc in the two cases zero and 4-amp. field. This was done by plotting $n_e r$ against $r$ and measuring the areas under the curves. The approximate symmetry of the curves made it permissible to average the data for positions 1 and 5 and for 2 and 4 and assume complete symmetry. This is theoretically justifiable to a first-order approximation.

The results are:

zero field $16.2\times10^{11}$ electrons/cm$^{-1}$
48.4 oersteds $17.9\times10^{11}$.

### d. Space potential distribution and arc gradient

In Fig. 9 are shown the space potential distributions across the diameter of the tube for the two cases of zero field and 48.4 oersteds. The smaller lateral mobility of the plasma electrons in a longitudinal magnetic field should decrease the plasma field necessary to maintain the balance between ion and electron currents to the wall. Consequently we should expect the curve for the magnetic field case to be flatter than for the zero field case. But a direct comparison of plasma fields can only be made for identical distributions of electron density. The peaking of the 48.4-oersted distribution would in itself require an increase of plasma field which would counteract any flattening tendency. It will appear below where the theoretical analysis is undertaken that a definite relative flattening

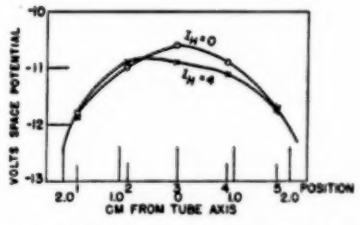


FIG. 9. Potential distribution across arc without and with magnetic field.

of the potential distribution has occurred. Had time permitted, a cross-section plot for the 4(20) case would have been made, for which a direct comparison of plasma fields would have been possible.

At zero field the longitudinal gradient was 0.33 v $cm^{-1}$. At $H=48.4$ oersteds the gradient decreased to 0.28 v $cm^{-1}$. Although the direction of change was in accordance with the predictions of the theory, it should be remarked (1) that the effect was much larger than expected, and (2) the deviation of the electron distribution in the cross section from the normal was probably of primary importance. The gradient of 0.32 v $cm^{-1}$ in the 4(20) case bears witness to this.

With increasing magnetic field the total arc drop was also observed to decrease. However, in the 4(20) case the total arc drop, like the gradient, had approximately its zero field value. As a matter of fact there is very little in these experiments to indicate a difference between the zero field and 4(20) cases. Table I summarizes these data.

### e. Electron temperature

Theory indicates that as the loss of carriers to the walls decreases with increasing magnetic field the electron temperature should decrease. The experimental results were complicated by unexplained variations. A résumé is given in Table II. It shows that a magnetic field did in fact lower $T_e$, but why it should be lower at probe 3 than at 2 is not known. Also, the lower gradient in the 4 compared to the 4(20) case, and the fact that the peaking in the former should make the fractional loss of carriers less are not consistent with the low $T_e$ in the latter case.

By using line intensities to determine electronic energy Rokhlin[2] was able to show that electron temperature decreased with increasing field. He worked with two vapor pressures of mercury, $0.9\times10^{-3}$ and $5.9\times10^{-3}$ min., but he does not state to which his electron energy results apply. His Fig. 14 shows a 15 to 20 percent drop in energy for 50 oersteds. As the present results are at complete variance with this, it is probable that his figure applies to the lower vapor pressure, which means that to obtain comparable results our field would have had to be about $50\times(5.4/0.9)=300$ oersteds. This is not inconsistent with the small change found by us.

TABLE I. *Values of arc gradient for different magnetic fields.*

| $I_H$ (amp.) | $X$(v $cm^{-1}$) | Total Drop (volts) |
|---|---|---|
| 0 | 0.33 | 32.7±0.3 |
| 2 | 0.31 | 30.9±0.6 |
| 4 | 0.28 | 29.7±0.4 |
| 4 (20) | 0.32 | 32.9±0.1 |

TABLE II. *Values of electron temperature.*

| Probe | $T_e$ | | |
|---|---|---|---|
| | $I_H=0$ | $I_H=4$ | $I_H=4(20)$ |
| No. 2 Position 3 | 19,200 | 18,700 | 18,200 |
| No. 2 $T_e$ averaged over positions 1 to 5 | 18,750 | 18,300 | |
| No. 3 | 18,200 | 17,400 | |

## V. Theory

In the presence of a longitudinal magnetic field, according to Tonks' theory, the Boltzmann equation $n_e=n_0\exp(-eV/kT)$ is to be replaced by the equation

$$n_e=n_0\exp(-eV/kT\tau), \tag{1}$$

where

$$\tau=\frac{\alpha D_e-\mu D_p}{\alpha D_e+\mu D_p T_e/T_p}<1, \tag{2}$$

in which $\mu$ is the ratio of radial drift velocity of electrons and ions.

Equation (1) can be written

$$\ln n_e=(-e/(kT\tau))V+\ln n_0. \tag{3}$$

A rough test of the theory is now possible inasmuch as a plot of $\ln n_e$ *vs.* $-V$ taken from Figs. 7 and 9 should give a straight line of slope $e/kT\tau$. From this a value of $\tau$ can be obtained and compared with the value calculated from Eq. (2). Figure 10 is a replot of the data in Figs. 7 and 9. From the $H=0$ curve, using 19,000° as the reasonable average value for $T_e$, $\tau_0=0.99$ which agrees with the theoretical value unity. For $H=48.4$ and with $T_e=18{,}300°$, $\tau_{48.4}=0.75$ which is significantly less than unity and shows a relative flattening of the potential distribution.

Before a value of $\tau$ can be computed from Eq. (2), a number of other quantities must be determined.

**a. Electron diffusion coefficient**

The electron diffusion coefficient $D_e$ can be found from known quantities by means of the equation for the arc current $i_z$:

$$i_z = e^2 N_e X D_e / kT_e. \quad (4)$$

Solving for $D_e$,

$$D_e = 5.39\times10^{14} i_z T_e / N_e X \text{ (practical units)}. \quad (5)$$

In the 48.4-oersted case

$$D_{eH} = \frac{5.39\times10^{14}\times4\times18{,}300}{1.79\times10^{12}\times0.28} = 7.87\times10^{7}.$$

In the zero field case

$$D_{e0} = \frac{5.39\times10^{14}\times4\times19{,}000}{1.62\times10^{12}\times0.33} = 7.66\times10^{7}.$$

The two calculations should give the same result, since the electronic motion to which the calculation applies is along the lines of force. The agreement is reasonably good.

**b. Determination of $\alpha$**

The constant $\alpha$ that appears in Eq. (2) is defined by the following relations.[7]

$$\alpha = \gamma_a \alpha_a, \quad (6)$$

$$\alpha_a = 1/(1+h'^2), \quad (7)$$

$$h' = 1.374\times10^{-4}(D_e H_z / T_e), \quad (8)$$

where $\gamma_a$ is a correction factor which for $H=48.4$ oersteds has the value 1.57.

Using $D_{eH}=7.87\times10^{7}$, $H_Z=48.4$ oersteds, $T_e=18{,}300°$, then $h'=0.591H_Z=28.6$,

$$\alpha = 1.92\times10^{-3}.$$

At zero field the value of $\alpha$ is, of course, unity.

**c. Positive ion diffusion coefficient $D_p$**

The ion current density to the wall affords a means to determine $D_p$. In view of the inexact nature of the arc theory it is probably more accurate to use the ion current equation in a form which involves $N_e$ rather than $n_0$, the axial electron density. In this form the ion current equation is[8]

$$I_p = 1.248\frac{\alpha D_e D_p (T_e+T_p) e N_e}{(\alpha D_e T_p' + \mu D_p T_e) 0.432\pi a^3}. \quad (9)$$

This can be solved for $D_p$.

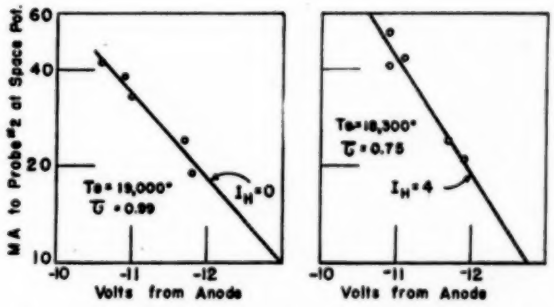


FIG. 10. Electron current density (proportional to electron density) against space potential across arc, showing departure from Boltzmann distribution with magnetic field.

In the absence of magnetic field $H=0$, $\alpha=1$, the value of $\mu$ is unimportant since the term in which it appears is negligible, $N_e=1.62\times10^{12}$, $a=2.3$, $D_{e0}=7.66\times10^{7}$, $T_e=19{,}000°$K, $T_p \leqq T_{po} \leqq 350°$K, $I_p=7.5\times10^{-4}$ amp. cm$^{-2}$ from measurement on probe No. 4. Then $D_{p0}=690$.

When $H=48.4$ oersteds, $\alpha=1.92\times10^{-3}$, $N_e=1.79\times10^{12}$, $D_{eH}=7.87\times10^{7}$, $T_e=18{,}500$, $T_p \leqq T_g \leqq 350$, $I_p=6.54\times10^{-4}$. There is some uncertainty about the value of $\mu$. The suppression of electron flow to the wall probe while the ion current was being measured made $\mu=0$ locally. Elsewhere, however, since the tube walls were insulating, $\mu=1$. Thus for the effective $\mu$ $0<\mu<1$ and it probably lies nearer unity. We find,

$$D_{pH}=720 \quad \text{for} \quad \mu=1,$$
$$D_{pH}=580 \quad \text{for} \quad \mu=0,$$

in good agreement with $D_{p0}$.

For the calculation of $\tau$ by Eq. (2) we have chosen $D_{pH}=690$ as a reasonable value and $\mu=1$ since the cylindrical probe measurements involved no unbalance between ion and electron currents to the walls. For the remaining quantities the 48.4-oersted case values were used. Then

$$\tau_{48.4} = \frac{1.92\times10^{-3}\times7.87\times10^{7} - 690}{1.92\times10^{-3}\times7.87\times10^{7} + 690\times18{,}300/350} = 0.80.$$

This is to be compared with the previously

[7] Equations (6), (7) and (8) are Eqs. (6) and (7) of reference 1.

[8] See Eq. (24.5) in reference 1.

obtained value 0.75. The agreement is as good as the accuracy of the experiments would lead us to expect.

## VI. Summary

The absence of a constricting effect in a *uniform* longitudinal magnetic field has been confirmed. The primary electrons from the cathode formed a collimated beam which bore the imprint of cathode structure and which disappeared rather abruptly into a general glow. "Abnormal" electron distributions were found to be transmitted with decreasing amplitude along the arc in the direction of the anode.

A magnetic field of 70 oersteds distorted probe characteristics at $5.4\times10^{-3}$ mm pressure so badly as to make them uninterpretable. Therefore attention was confined to a 50-oersted field. The stable cross-sectional distribution of electron density was the same with this field as without field and a distribution which differed from the "normal" tended to become normal in the direction of the anode.

The abnormal distribution was found to obey a modified Boltzmann distribution in accordance with the theory of an arc in a longitudinal field.

Unfortunately the magnetic field distortion of the probe characteristics began in the range where the effects on the arc were just becoming large enough to exhibit significant differences from the zero field condition. As a consequence the experimental results did not exhibit the magnetic effects as vividly as could be wished and the test of the theory was a rather mild one.

MARCH 15, 1941 PHYSICAL REVIEW VOLUME 59

# Transmission of an Electron Density Disturbance Along a Positive Column in a Longitudinal Field

Lewi Tonks
*Research Laboratory, General Electric Company, Schenectady, New York*
(Received November 28, 1940)

The distribution of ions and electrons in the cross section of a uniform positive column is maintained by the radial motions of these particles. This distribution is designated as "normal." A disturbance of this distribution at some point in the column is followed on the anode side by an asymptotic approach to the normal. In the absence of a longitudinal magnetic field the recovery of a normal distribution occurs within a very short distance, but a longitudinal magnetic field slows down the readjustment by decreasing the radial mobility of the electrons. By making certain simplifying assumptions a theory for the approach of a disturbed column back to normal when the disturbance is cylindrically symmetrical has been worked out. The distribution is developed in a series of zero order Bessel functions, and it is found that the first term, which corresponds to the normal distribution, approaches a constant amplitude along the column whereas successive terms have successively greater space decrements. The decrement of the $i$th term approaches the constant value

$$\frac{(x_i^2-x_1^2)\alpha(T_e+T_p)}{(1-\alpha)T_e a^2(-\epsilon)},$$

where $x_i$ is the $i$th root of $J_0(x)=0$, $\alpha$ is the factor giving the reduction in transverse electron mobility, $T_e$ and $T_p$ are the electron and positive ion temperatures, $a$ is the radius of the column and $\epsilon$ is $(e/kT_e)(\partial V/\partial z)$. When compared with the experimental results of Cummings and Tonks, the theory calls for a reduction of the second term of the series expansion to 50 percent in 12.5 cm of arc length whereas experiment gave 33 percent.

## 1. Introduction

IN the uniform positive column of a low pressure discharge there is a *normal* distribution of electron (and ion) density in the cross section which maintains a balance, in each element of volume, between the new ions and electrons formed there and the net rate at which these particles escape radially under the influence of the electric fields and concentration gradients. The net longitudinal outflow is zero because of the axial uniformity of the arc. Such a normal distribution exists whether the column be in a finite uniform magnetic field or none at all but the distribution will of course be different depending on the orientation and strength of the

magnetic field. Experiment[1] indicates in agreement with theory[2] that the normal distributions for no field and for uniform longitudinal field are identical.

With no field the distribution reaches the normal in very short distances, evidence of which is found in the uniformity of the positive column even close to the cathode or to the point where a change in column diameter occurs. This does not mean that deviations from the normal electron *temperature* may not extend along the column for some distance, but that the charge reaches its normal distribution quite promptly.

The presence of a longitudinal magnetic field, however, reduces the transverse mobility of the electrons and thus decreases the ease with which an abnormal distribution disappears. The electrons, moving longitudinally with ease and transversely with difficulty, propagate the maldistribution along the column. Such effects have been definitely found in experiments on a mercury arc column reported by C. S. Cummings and L. Tonks.[1] It therefore becomes of interest to analyze the problem theoretically to gain, if possible, a quantitative understanding of the phenomenon. The problem is that of dealing with a non-uniform column in which longitudinal transfer of ions and electrons do play a part.

## 2. *A Priori* Limitations of the Theory

The present application of the theory will be only to the case for which the plasma extends to within a short distance of the tube wall. The wall sheath is supposed to be thin, so that the positive ions originating in the plasma flow freely to the walls. Any case in which the column has been pulled away from the wall, as by a sharply increasing magnetic field, a constriction in the arc tube, or by a cathode of limited area brings in factors which will not be considered here. The present treatment is concerned rather with what goes on beyond the point at which such a constricted column first expands to fill the whole cross section.

The theory to be developed will suffer from one of the same errors as the present theory of the positive column, namely that arising from the assumption that the ions drift with a velocity proportional to the electric field. We know that in the range of pressures and fields which exist in the plasma their motion is more nearly proportional to the square root of the field.[3] But such a law would result in nonlinear equations whose solution would be practically impossible. Only disturbances which have cylindrical symmetry will be treated because it has not been found possible to solve the equations which include azimuthal variation.

Other limitations of the theory, which are consequences of mathematical necessity, will appear as the theory is developed.

## 3. The Fundamental Equations

For definiteness let the positive $z$ direction be toward the anode so that it is the direction of electron drift.

As usual, equality of electron and positive ion densities $n_e$ and $n_p$, respectively, is assumed:

$$n_e = n_p, \tag{1}$$

so that where necessary these quantities can be used interchangeably and the subscripts can be dropped.

There are six other equations which form the system which will be used to describe the behavior of the plasma. The first four are the drift equations for the transverse ($u$) and longitudinal ($w$) drift velocities of the electrons (subscript $e$) and ions (subscript $p$):

$$u_e = -\alpha D_e\left(\frac{\partial n_e}{n_e \partial r} + \frac{e}{kT_e}\frac{\partial V}{\partial r}\right), \tag{2}$$

$$u_p = -D_p\left(\frac{\partial n_p}{n_p \partial r} - \frac{e}{kT_p}\frac{\partial V}{\partial r}\right), \tag{3}$$

$$w_e = -D_e\left(\frac{\partial n_e}{n_e \partial z} + \frac{e}{kT_e}\frac{\partial V}{\partial z}\right), \tag{4}$$

$$w_p = -D_p\left(\frac{\partial n_p}{n_p \partial z} - \frac{e}{kT_p}\frac{\partial V}{\partial z}\right). \tag{5}$$

Here $D_e$ and $D_p$ are electron and ion diffusion coefficients in the absence of magnetic field and $\alpha$ is the fraction giving the decrease of transverse electron mobility due to the magnetic field.[2]

[1] C. S. Cummings and L. Tonks, preceding paper.
[2] L. Tonks, Phys. Rev. **56**, 360 (1939).
[3] K. H. Kingdon and E. J. Lawton, Phys. Rev. **56**, 215 (1939).

The other two equations are those of continuity for electrons and ions, respectively:

$$\frac{\partial(n_e u_e r)}{r\partial r}+\frac{\partial(n_e w_e)}{\partial z}=\lambda n_e, \tag{6}$$

$$\frac{\partial(n_p u_p r)}{r\partial r}+\frac{\partial(n_p w_p)}{\partial z}=\lambda n_e, \tag{7}$$

$\lambda$ being the rate of production of ion-electron pairs per electron per second.

Even on the simplest theoretical grounds another relation giving the relation between $\lambda$ and the arc gradient should be included. Our knowledge of this relationship is meager, however. In addition, its introduction would create great mathematical difficulties, and there is a sufficiently satisfactory detour around this complication, which will be introduced later.

Finally, besides the usual boundary condition that $n$ be zero at the tube wall, we must seek a solution in which (1) $\partial V/\partial z$ becomes constant for large enough $z$ and (2) the wall current is small so that the total arc current does not change rapidly along the arc length.

## 4. Necessary Approximations

In order to solve the six equations in convenient form it is necessary to make certain simplifications. First, we shall assume that the "partial" drift arising from longitudinal diffusion is small compared to that arising from the electric field so that the quantities $\partial n/n\partial r$ may be dropped from Eqs. (4) and (5). If the diffusion terms are left in these equations, a $\partial^2 n/\partial z^2$ term appears later in Eq. (11) which makes the solution under the assumed conditions far more difficult.

Second, we assume that the arc gradient is essentially constant, an assumption that will be connected with the question of the relation between $\lambda$ and $\partial V/\partial z$.

The various simplifications result in the following two equations as a consequence of substituting Eqs. (2) to (5) into Eqs. (6) and (7):

$$-\alpha D_e\nabla_r^2 n-\alpha D_e\frac{\partial}{r\partial r}\left(rn\frac{\partial\eta}{\partial r}\right)-D_e\epsilon\frac{\partial n}{\partial z}=\lambda n, \tag{8}$$

$$-D_p\nabla_r^2 n+\frac{D_pT_e}{T_P}\frac{\partial}{r\partial r}\left(rn\frac{\partial\eta}{\partial r}\right)+\frac{D_pT_e}{T_P}\epsilon\frac{\partial n}{\partial z}=\lambda n, \tag{9}$$

where $\nabla_r^2$ is the Laplacian with respect to $r$ only, and

$$\eta=eV/kT_e, \quad \epsilon=\partial\eta/\partial z. \tag{10}$$

Note that $\epsilon$ is intrinsically negative for electron flow toward the anode.

These equations contain the two dependent variables $n$ and $\eta$. Multiplying the first by $D_pT_e/T_p$, the second by $\alpha D_e$ and adding gives

$$\nabla_r^2 n+P\partial n/\partial z+Q\lambda n=0 \tag{11}$$

with

$$P=\frac{(1-\alpha)T_e\epsilon}{\alpha(T_e+T_p)}, \tag{12}$$

$$Q=\frac{\alpha D_eT_p+D_pT_e}{\alpha D_eD_p(T_e+T_p)}. \tag{13}$$

The form of Eq. (11) suggests zero-order Bessel functions as appropriate solutions. It is already known that the function whose first root lies at the wall, namely $J_0(2.40\ r/a)$, is the solution when $\partial n/\partial z$ is zero. This normal solution, as has already been stated, just balances the net radial outflow of ions and electrons from each elementary volume against the creation of new particles. As a consequence, $N$, the number of electrons per cm length of arc, which is given by

$$N=2\pi\int_0^a nrdr \tag{14}$$

is constant.

Now it is obvious that any distribution other than the normal will fail to maintain such a balance. For example, a distribution in which the relative concentration at the axis is larger would result in a slower escape of electrons and hence an increase in $N$ toward the anode. The constancy of the arc current then would require that the gradient decrease, and this in turn would cause a decrease in $T_e$ and $\lambda$, thus bringing compensating factors into play. The faster $\lambda$ changes with $T_e$, the smaller would be the actual changes in $T_e$ and $\epsilon$ which would accomplish the compensation. Actually $\lambda$ varies rapidly with $T_e$,

and for present purposes it will be assumed that this variation is so great as to bring about complete compensation with only infinitesimal, and hence negligible, changes in $T_e$ and $\epsilon$. Accordingly $\lambda$ is to be treated as a function of $z$ in Eq. (11), and is to be determined by the condition that $N$ remain constant, if there is no net current to the wall, or by the actual variation in $N$ which is consistent with a wall current.

## 5. Solution of the Equations*

We suppose that the actual charge distribution is analyzed by a Bessel-Fourier analysis into the sum of a set of Bessel function distributions, each with its unique dependence on $z$, represented by $Z_i$:

$$n=\sum_{i=1}^{i=\infty} n_i J_0\left(\frac{x_i r}{a}\right) Z_i. \tag{15}$$

Here $x_i$ is the $i$th root of $J_0(x)=0$ so that the wall-boundary condition, $n=0$, is automatically fulfilled. If each term in the series of Eq. (15) satisfies Eq. (11), substitution reveals that

$$n=\sum n_i J_0\left(\frac{x_i r}{a}\right) \exp\left[P^{-1}\int_0^z\left(\frac{x_i^2}{a^2}-Q\lambda\right)dz\right], \tag{16}$$

where, as has been remarked, $\lambda$ is a function of $z$.

With insulating walls $N$ is constant, so that

$$0=\frac{\partial N}{\partial z}=\frac{2\pi\partial}{\partial z}\int_0^a nr\,dr$$

$$=2\pi a^2 \exp\left[\int_0^z \frac{-Q\lambda}{P}dz\right]\sum\frac{n_i}{x_i}\left(\frac{x_1^2}{a^2}-Q\lambda\right)$$

$$\times J_1(x_i)\exp\left(\frac{x_i^2 z}{a^2 P}\right)$$

and solving for $\lambda$:

$$a^2 Q\lambda=\frac{\sum n_i x_i J_1(x_i)\exp(x_i^2 z/a^2P)}{\sum n_i x_i^{-1}J_1(x_i)\exp(x_i^2 z/a^2P)}. \tag{17}$$

Turning now to the transverse gradient in the column, Eq. (16) is to be substituted into either Eq. (8) or (9) giving

$$\frac{D_e D_p(T_p+\alpha T_e)x_i^2-a^2\lambda(D_eT_p+D_pT_e)}{aD_eD_pT_e(1-\alpha)}$$

$$\times\sum\frac{n_i'}{x_i}J_1\left(\frac{x_i r}{a}\right)+n\frac{\partial\eta}{\partial r}=0, \tag{18}$$

where

$$n_i'=n_i\exp\left[P^{-1}\int_0^z\left(\frac{x_i^2}{a^2}-Q\lambda\right)dz\right], \tag{19}$$

is the amplitude of the $i$th partial distribution at the axial distance $z$.

## 6. Interpretation

The reasonable expectation is that the amplitude of each of the partial distributions, except the normal, will decrease with distance, and that the normal will approach a constant value. It will now appear that the solution describes just such behavior. It is necessary that $\partial n/\partial r$ shall be negative or zero at $r=a$. At $z=0$, then,

$$0\geqq\partial n/\partial r|_a=-a^{-1}\sum n_i x_i J_1(x_i),$$

which assures a positive or zero numerator in the right member of Eq. (17). The denominator, being proportional to $N$, is positive. It follows that $\lambda$ is initially positive or zero. Now each successive term in the two sums decreases more rapidly than the last because of the increase in $x_i$ from term to term and the fact that $P$ is negative. This assures that even if $\lambda$ was initially zero, it becomes and remains positive as $z$ increases, and approaches the limiting value

$$\lambda\rightarrow x_1^2/a^2Q. \tag{20}$$

Examination of Eq. (16) then shows that the normal ($i=1$) term of the sum approaches constancy, whereas every subsequent term decreases with a variable "absorption coefficient" $\gamma_i$ which approaches the value $-(x_i^2-x_1^2)/a^2P$.

Using Eq. (12) we have

$$\gamma_i\rightarrow(x_i^2-x_1^2)\frac{\alpha(T_e+T_p)}{(1-\alpha)T_e a^2(-\epsilon)}. \tag{21}$$

From Bessel function tables it is found that the coefficients for successive $\gamma$'s have the values:

| $i$: | 2 | 3 | 4 |
|---|---|---|---|
| $(x_i^2-x_1^2)$: | 24.7 | 69.0 | 133.3 |

* I am indebted to Dr. A. V. Hershey for valuable help in solving the differential equations.

## 7. Limitations of the Solution

For zero magnetic field $\alpha$ is unity and Eq. (21) becomes meaningless. As this condition is approached by decreasing the magnetic field the limiting values of the $\gamma$'s become so large that the original neglect of longitudinal diffusion is seen to be no longer justified. This approximation therefore limits the validity of the present analysis to cases where the magnetic field is not too small. Since the longitudinal diffusion is relatively more important for the higher order components of the disturbance, the analysis is also limited in that direction and ceases to apply for values of $i$ that are too great.

The more crucial of the two places where diffusion has been neglected is in Eq. (4). There the assumption was that

$$1 \ll \frac{\epsilon}{n_i^{-1}\partial n_i/\partial z} = \frac{(1-\alpha)T_e\epsilon^2}{\alpha(T_e+T_p)(x_i^2/a^2-Q\lambda)}.$$

As this condition is chiefly of interest for $i$ greater than unity the particular value of $\lambda$ used makes little difference. We therefore choose its limiting value from Eq. (20). Since $T_e+T_p \backsimeq T_e$, the condition becomes

$$\frac{(1-\alpha)\epsilon^2 a^2}{\alpha(x_i^2-x_1^2)} \gg 1. \tag{22}$$

## 8. Theory for Non-Insulating Walls

The case to which attention has been confined so far is that in which the arc current remained constant along the length of the column, that is, the case of insulating walls which impose the condition that $u_e=u_p$ at the wall. Equation (11) was derived, however, without any such assumption, so that it is valid even when a net wall current flows. Only $\lambda$ depended on that assumption, so that a change in $\lambda$ should take care of its abandonment.

To apply the theory to this case we assume that the cross section distribution is normal so that $n_2$, $n_3$, etc. are zero. Any other assumption presents great complications. Also, for simplicity, we suppose that the current variation is exponential, that is, in terms of $N$,

$$N=N_0\epsilon^{\beta z}. \tag{23}$$

Comparison with Eq. (16) shows that

$$x_1^2/a^2-Q\lambda=P\beta. \tag{24}$$

If now this is used to eliminate $\lambda$ from Eq. (18) we find that

$$\frac{\partial\eta}{\partial r}=\tau_a\frac{x_1J_1(x_1r/a)}{aJ_0(x_1r/a)}, \tag{25}$$

where

$$\tau_a=\frac{\alpha D_e-D_p+a^2x_1^{-2}\beta(-\epsilon)(D_e+D_pT_e/T_p)}{\alpha D_e+D_pT_e/T_p}. \tag{26}$$

Integration of Eq. (25) gives

$$J_0(x_1r/a)=\epsilon^{-\eta/\tau a}, \tag{27}$$

a result of the same form as has already been derived[2] without considering longitudinal effects.

These results, of course, are consistent with the continuity of current in the arc and to the walls. A calculation to demonstrate this simply serves as a check on the mathematics and tells us nothing new.

We can, however, confirm a previous assumption[2] that the ratio of $u_e$ to $u_p$ is a constant over the cross section of the column under these conditions. From Eqs. (2) and (3):

$$u_e=-\alpha D_e x_1(\tau_a-1)J_1(x_1r/a)/aJ_0(x_1r/a),$$
$$u_p=-D_p x_1(1+\tau_aT_e/T_p)J_1(x_1r/a)/aJ_0(x_1r/a)$$

with the previous definition of $\mu$,[2]

$$\mu=\frac{u_e}{u_p}=\frac{\alpha D_e(1-\tau_a)}{D_p(1+\tau_aT_e/T_p)}, \text{ a constant,} \tag{27}$$

and the previously given value for $\tau_a$ ($\tau$ in the reference) is confirmed:

$$\tau_a=\frac{\alpha D_e-\mu D_p}{\alpha D_e+\mu D_pT_e/T_p}. \tag{28}$$

## 9. Comparison with Theory

The only experimental results which are available for comparison with this theory are those of Cummings and Tonks. Their Fig. 8 shows the approach to a normal distribution with increasing $z$ of a distribution which was initially peaked at the axis. We assume that of the abnormal partial distributions, only $n_2$ is appreciable and that in the range shown $\gamma_2$ is a constant.

It would be simplest if the 47-ma normal distribution contained the same total number of electrons as the abnormal distribution. Then it could be shown,[4] in terms of the values in the figure, that

$$\epsilon^{-12.5\gamma_2}=(51-47)/(59-47)$$

whence

$$\gamma_2=0.088.$$

We know, however, that $N$ for the 59-ma plasma is 10 percent greater than for the 47-ma plasma.[1] But since this difference is itself proportional to the magnitude of $n_2$, it will be proportionately less with increasing $z$ so that the above result is not affected.

To calculate $\gamma_2$ from Eq. (21) we take the following values from Cummings and Tonks: $T_e=18{,}500°\text{K}$, $T_p=350°\text{K}$, $\alpha=1.92\times10^{-3}$, $a=2.3$ cm, $-\epsilon=0.28\times11{,}600/18{,}500$. It follows that

$$\gamma_2=0.052.$$

The agreement, though not close, is reasonable in view of theoretical approximations and experimental uncertainties.

Finally, it is necessary to find to what degree the condition of (22) is fulfilled. It appears that the left member has the value 3.4 for the $n_2$ distribution and would be only 1.2 for the $n_3$. Therefore the neglect of the diffusion term from Eq. (4) introduces considerable inexactness in the present calculation, and the analysis becomes exact only when larger magnetic fields giving considerably smaller values of $\alpha$ are used.

[4] See Appendix.

## Appendix

Calculation of absorption coefficient of second partial distribution from axial concentration measurements.

Let $n_f$ = axial concentration at first point, with field.
$n_s$ = ditto second point.
$n_0$ = axial concentration with no field but for same total charge in cross section.
$n_1$ = axial concentration of first partial distribution at first point.
$n_2$ = ditto second partial at first point.
$n_1'$ = ditto first partial at second point.
$n_2'$ = ditto second partial at second point.
$f=\epsilon^{-\gamma_2 z}$ = fractional decrease in second partial between points.

Equating total charges in the cross section gives,

$$n_1J_1(x_1)/x_1-n_2J_1(x_2)/x_2=n_0J_1(x_1)/x_1,$$
$$n_1'J_1(x_1)/x_1-n_2'J_1(x_2)/x_2=n_0J_1(x_1)/x_1.$$

The axial concentrations at first and second points are:

$$n_1+n_2=n_f;\quad n_1'+n_2'=n_s.$$

By definition, $n_2'=fn_2$. By using the last equation to eliminate $n_2'$ and substituting $\lambda$ for $x_1J_1(x_2)/x_2J_1(x_1)$:

$$n_1-\lambda n_2=n_1'-\lambda fn_2=n_0,$$
$$n_1+n_2=n_f,\quad n_1'+fn_2=n_s.$$

From these

$$n_s-n_0=f(1+\lambda)n_2;\quad n_f-n_0=(1+\lambda)n_2,$$

whence

$$f=(n_s-n_0)/(n_f-n_0)=\epsilon^{-\gamma_2 z}.$$

# Letters to the Editor

*PROMPT publication of brief reports of important discoveries in physics may be secured by addressing them to this department. Closing dates for this department are, for the first issue of the month, the eighteenth of the preceding month, for the second issue, the third of the month. Because of the late closing dates for the section no proof can be shown to authors. The Board of Editors does not hold itself responsible for the opinions expressed by the correspondents.*

*Communications should not in general exceed 600 words in length.*

## Dislocations and Magnetization

WILLIAM FULLER BROWN, JR.
*Palmer Physical Laboratory, Princeton University, Princeton, New Jersey*
February 27, 1941

THE writer recently suggested[1] that line concentrations of force might be responsible for the term $a/H$ in the empirical formula for the magnetization curve of nickel at high fields, $J=J_s-a/H-b/H^2+CH$, and tentatively identified these line concentrations with the "dislocations" of plasticity theory. The following approximate calculation, based directly on dislocation theory, shows that both the occurrence of the $a/H$ term and the increase of $a$ and $b$ with plastic strain may be attributed to internal stresses produced by the dislocations.

Let $Oy$ be the direction of the field and of the specimen axis, $Oz$ the direction of the dislocation lines (radially outward from the axis in the region under consideration), and $Ox$ the direction of slip; this is roughly the situation in a twisted wire. If $\alpha=\cos(\mathbf{J}, x)$ is small, the magnetostrictive energy density[2] for a specimen with saturation magnetostriction $-\lambda_\infty$ is $3\lambda_\infty X_y\alpha$. The shearing stress $X_y$ at a distance $r$ from a dislocation[3] is $\lambda_0 G'\phi(\theta)/\pi r$, where $\lambda_0$ is the distance between atoms along $Ox$, $G'\leqq$the rigidity, and $\phi(\theta)$ is an angular factor. For a single dislocation, therefore, $\alpha$ varies in the $xy$-plane in accordance with the equation[1]

$$\nabla^2\alpha-\eta\alpha=k\phi(\theta)/r, \tag{1}$$

where $k=3\lambda_\infty G'\lambda_0/\pi C$, $\eta=HJ_s/C$; $C\leqq 10^{-5}$ erg/cm measures the strength of the interatomic coupling forces. Transformation to the dimensionless variable $v=\eta^{\frac{1}{2}}r$ shows that

$$\alpha=k\eta^{-\frac{1}{2}}f(v,\theta), \tag{2}$$

where the function $f$ is dimensionless.

For $n$ dislocations per cm², distributed at random, $1-J/J_s$ is found by integrating $\frac{1}{2}\alpha^2$ over the $xy$-plane and multiplying by $n$. Since $dxdy=\eta^{-1}vdvd\theta$, the result is $c_1\pi nk^2/\eta^2$, where $c_1=\int\!\!\int f^2 vdvd\theta/2\pi$ is a numerical constant; or $J_s-J=b/H^2$, with

$$b=(9c_1/\pi)n(\lambda_\infty G'\lambda_0)^2/J_s. \tag{3}$$

This may be rewritten

$$J/J_s=1-c_1'(\lambda_\infty\sigma_i/HJ_s)^2, \tag{4}$$

with

$$\sigma_i=c_2G'\lambda_0\sqrt{n}, \tag{5}$$

where $c_1'$ and $c_2$ are numerical constants. Equation (4) is identical with that given by the Becker-Kersten rotation theory[2] for "internal stress" $\sigma_i$; Eq. (5) suggests that $\sigma_i$ may be identified with the stress produced by the dislocations in Taylor's theory of hardening.[3] In Becker's theory $c_1'\leqq\frac{3}{8}$, and in Taylor's $c_2\leqq\frac{1}{3}$. If the tentative value $9c_1/\pi=c_1'c_2^2=3/125$ is inserted in Eq. (3), $n$ may be calculated from Kaufmann's data on the increase of $b$ with plastic twist.[4] The result is $n/\gamma\leqq 10^{12}$ dislocations per cm² per unit of plastic shear ($\gamma$), in agreement with the value calculated from purely mechanical data by Taylor's theory.[1]

Dislocations are of two signs, and opposite kinds attract each other toward a common value of $x$. They therefore tend to form pairs separated by a short distance $l$ parallel to $Oy$. The value of $\alpha$ for such a doublet may be found by applying the operator $-l\partial/\partial y$ to the right member of Eq. (2); it is of the form $\alpha=klg(v,\theta)$. For $n'$ doublets per cm², $J_s-J=a/H$, with $a=(9c_3/\pi)n'l^2(\lambda_\infty G'\lambda_0)^2/C$. If $n'\leqq n$ and $10^{-2}\leqq 9c_3/\pi\leqq 1$, Kaufmann's values of $a$ give $10^{-5}$ cm $\geqq l\geqq 10^{-6}$ cm; thus $l$ is less than the mean distance between dislocations but considerably greater than the interatomic distance—a plausible result.

It has been assumed here that the integrals $c_1$ and $c_3$ converge. Actually $c_1$ diverges logarithmically at $v=\infty$; in the rigorous theory $b$ is not exactly constant, but contains a logarithmic term in $H$.

[1] W. F. Brown, Jr., Phys. Rev. **58**, 736 (1940).
[2] R. Becker and W. Döring, *Ferromagnetismus* (Springer, Berlin, 1939), p. 146; pp. 167–8, 175.
[3] G. I. Taylor, Proc. Roy. Soc. **A145**, 362 (1934); J. M. Burgers, Proc. K. Ned. Akad. Wet. **42**, 293 (1939), especially pp. 305–6.
[4] A. R. Kaufmann, Phys. Rev. **57**, 1089A (1940) and private communication.

## Rotational Analysis, Perturbation and Predissociation in the CD and CH Bands

L. GERÖ AND R. F. SCHMID
*Physical Institute, Royal Hungarian University for Technical and Economic Sciences, Budapest, Hungary*
January 17, 1941

IN strongly condensed high frequency electric discharges through vapors of deutero-paraffin and ordinary benzol under various pressures, the entire CD and CH spectrum was photographed with a grating spectrograph of high dispersion and good resolution.

Rotational analysis of the CD bands in the region of 3150A has been made and the branches of the bands (0,0), (1,1) and (2,2) were followed up to $K'=39(v'=0)$, $K'=34(v'=1)$ and $K'=27(v'=2)$, where predissociation of the $C^2\Sigma^-$ state occurs. The corresponding predissociation in the CH bands has been suspected[1] and we found confirmation by observing the effect at $K'=26(v'=0)$ and $K'=21(v'=1)$ on the $C^2\Sigma^-$ state of CH.

A comparison of the predissociation effects on the 4300A CD and CH bands completes the findings of a previous paper,[1] based on pictures of CH bands alone, as follows: The $A^2\Delta\rightarrow X^2\Pi$ bands show *two* predissociation phenom-

ena. The lower one—corresponding to the effect on the $B^2\Sigma^+ \rightarrow X^2\Pi$ bands, observed by Shidei[2]—takes place at $K'>33$ for CD and $K'>23$ for CH on the $v'=0$, i.e., at $K'>25$ for CD and $K'>13$ for CH on the $v'=1$ vibrational level of the $A^2\Delta$ state and affects rather more the $F_{1e}$ sublevel sets. The upper one cuts the rotational sets with $K'>36$ for CD and $K'>26$ for CH on the $v'=0$, i.e., with $K'>29$ for CD and $K'>17$ for CH on the $v'=1$ level of the $A^2\Delta$ state.

As has been pointed out[3] on the basis of Shidei's measments,[2] the relative positions of the band origins in the $A^2\Delta \rightarrow X^2\Pi$ systems of CD and CH cannot be explained by the usual vibrational isotopic shifts and a perturbation of the $A^2\Delta$ state was suspected, the perturbing state being of the same $^2\Delta$ symmetry. This is confirmed now by constructing the $(B'-B'')$ curves[4] for all the carefully analyzed bands of the $A^2\Delta \rightarrow X^2\Pi$ system. The shape of the perturbations suggests that the convergence limit of the perturbing $^2\Delta$ state must lie rather low.

The spin-doublet separation of the $X^2\Pi$ ground state decreases with increasing quantum numbers for CD more rapidly than for CH and vanishes in the regions $8<K<16$ for CD, i.e., $13<K<18$ for CH on the $c$ sublevels and $9<K<23$ for CD; also $16<K<24$ for CH on the $d$ sublevels of the $\Lambda$-type doublet components. Above these regions a reversed splitting, increasing with $K$, sets in. The relative intensity, before they merge, of the lines having these new doublets as lower states differs markedly from that of the ordinary spin-doublets; the violet components are explicitly weaker, especially in the $Q$ branches of the two $^2\Sigma \rightarrow ^2\Pi$ systems. This circumstance and the unequal splittings at the same $K$ of the $c$ and $d$ sublevels explains now the observations of earlier workers[5] on the 3900A CD bands showing a semi-singlet structure at medium and higher rotational quantum numbers.

[1] L. Gerö, Physica **7**, 155 (1940).
[2] T. Shidei, Jap. J. Phys. **11**, 23 (1936).
[3] L. Gerö and R. Schmid, Zeits. f. Physik **115**, 47 (1940).
[4] R. Schmid and L. Gerö, Ann. d. Physik **33**, 70 (1938).
[5] A. McKellar and Ch. A. Bradley, Jr., Phys. Rev. **47**, 787 (1935).